ESA - MOST Dragon 2 Programme
2011 DRAGON 2 SYMPOSIUM
中国科技部-欧洲空间局合作 “龙计划”二期
“龙计划”二期2011年学术研讨会

Topographic Measurement

Annual Report of ID 5297

Mingsheng Liao

LIESMARS, Wuhan University

European Partners

- **Prof. Fabio Rocca (PI)**
- **Dr. Daniele Perissin (Co-PI)**
  Dipartimento di Elettronica ed Informazione
  Politecnico di Milano (POLIMI), Italy

- **Young scientists in Milan:**
  Mr. Guido Gatti, Research Assistant, POLIMI

Chinese Partners

- **Prof. Deren LI (PI)**
  Prof. Mingsheng LIAO (Co-PI), LIESMARS, Wuhan University
- **Mr. Hanmei WANG, Shanghai Institute of Geology Survey**

- **Young scientists in Wuhan and Shanghai:**

  Dr. Lu Zhang, Asso. Prof. , LIESMARS, Wuhan University
  Dr. Timo Balz, Post Dr. Fellow , LIESMARS, Wuhan University
  Ms. Yuanyuan Pei, Ph. D student of LIESMARS, Wuhan University
  Mr. Houjun Jiang, Ph. D student of LIESMARS, Wuhan University
  Ms. Lianhuan Wei, MSc student of LIESMARS, Wuhan University
  Mr. Zhilei Fang, Engineer, Shanghai Institute of Geology Survey

Project Objectives

Based on the fruitful results of Dragon-1, the scientific investigations focus on:

- Topographic mapping
- Monitoring Subsidence and landslide

Young Scientists' Activities

• **Young scientist team of LIESMARS had a meeting with Prof. Fabio Rocca in Beijing, during the Advanced SAR Conference, April 2011.**

• **Young scientist, Dr. Lu ZHANG, studied in ESRIN/ESA for 6-month training and research program**

Presented report for ESRIN and published paper in ISPRS Journal.

=> detailed description to be addressed in next presentation…

Young Scientists' Activities

- One PhD student participated the Training Course of Land Remote Sensing in Lanzhou, 2010.
- One PhD student of the joint program, Teng WANG, has completed his thesis defense in WHU and POLIMI, June 2010.
- Several co-authored papers were published.

Recent Publications

BOOK:

- **Time Series InSAR Analysis over the Three Gorges Region Techniques and Applications,** *Teng Wang, Mingsheng Liao and Fabio Rocca，VDM Verlag Publishing, Germany, September，2010.*

JOURNAL PAPERS:

- **Landslide Monitoring with High-Resolution SAR Data in the Three Gorges Area,**

  Mingsheng Liao, Jin Tang, Teng Wang, Timo Balz, Lu Zhang, **=>** *Science in China, accepted.*

- **Monitoring the stability of Three Gorges Dam with time-series technique,** *Teng Wang, M. Liao, D. Perissin, and F. Rocca* **=>** *Science in China, May, No. 5, 2011.*

- **Rational function modeling for spaceborne SAR datasets,** *Lu Zhang , Xueyan He, Timo Balz, Xiaohong Wei and Mingsheng Liao,* **=>** *ISPRS Journal of Photogrammetry and Remote Sensing, Vol. 66, No. 1, 2011*

- **Time Series InSAR Applications Over Urban Areas in China, Daniele Perissin and Teng Wang**

  => *IEEE Journal of Selected Topics in Earth Observations and Remote Sensing, 2011.*

Research Activities and Results

(May 2011 – June 2011)

Methodology

From conventional D-InSAR to PS-InSAR

Multi-temporal imaging

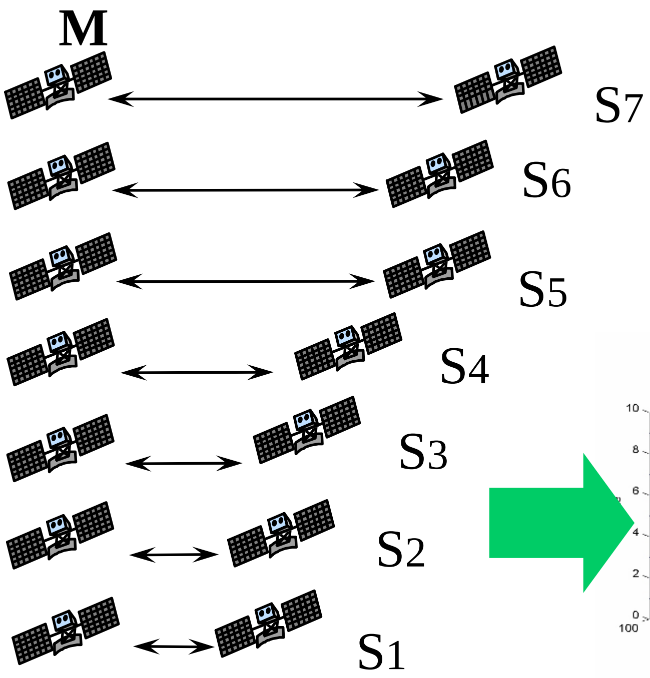

Image stack

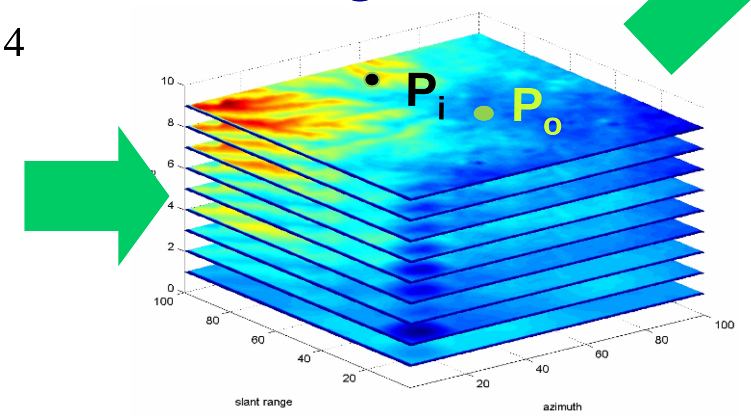

Subsidence vel.

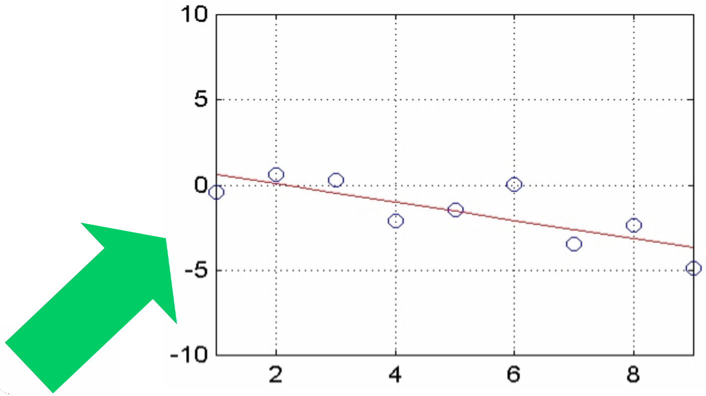

Components of interferometric phase

$$\phi_{ifg}^{k}(x_i) = \phi_{topo}^{k}(x_i) + \phi_{defo}^{k}(x_i) + \phi_{atmos}^{k}(x_i) + \phi_{orbit}^{k}(x_i) + n_{noise}^{k}(x_i)$$

Topographic phase	Displacement phase	Atmosphere phase	Orbit phase	Noise phase

Spatially correlated;
Temporally correlated

Spatially uncorrelated;
Temporally uncorrelated

Spatially correlated;
Temporally uncorrelated

Caused by the DEM error;
Spatial uncorrelated

$$-\frac{4\pi}{\lambda}\cdot\frac{B_{\perp}^{k}}{R^{k}\cdot\sin\theta^{k}}h_{error}(x_i)$$

$$= \beta^{k}\cdot h_{error}(x_i)$$

Spatially low-pass filter $\tilde{\varphi}_{x,i}$

3-D phase unwrapping - Temporal unwrapping

Estimate the best-fitted integer ambiguities and displacement components by Least-Square Estimator in temporal dimension

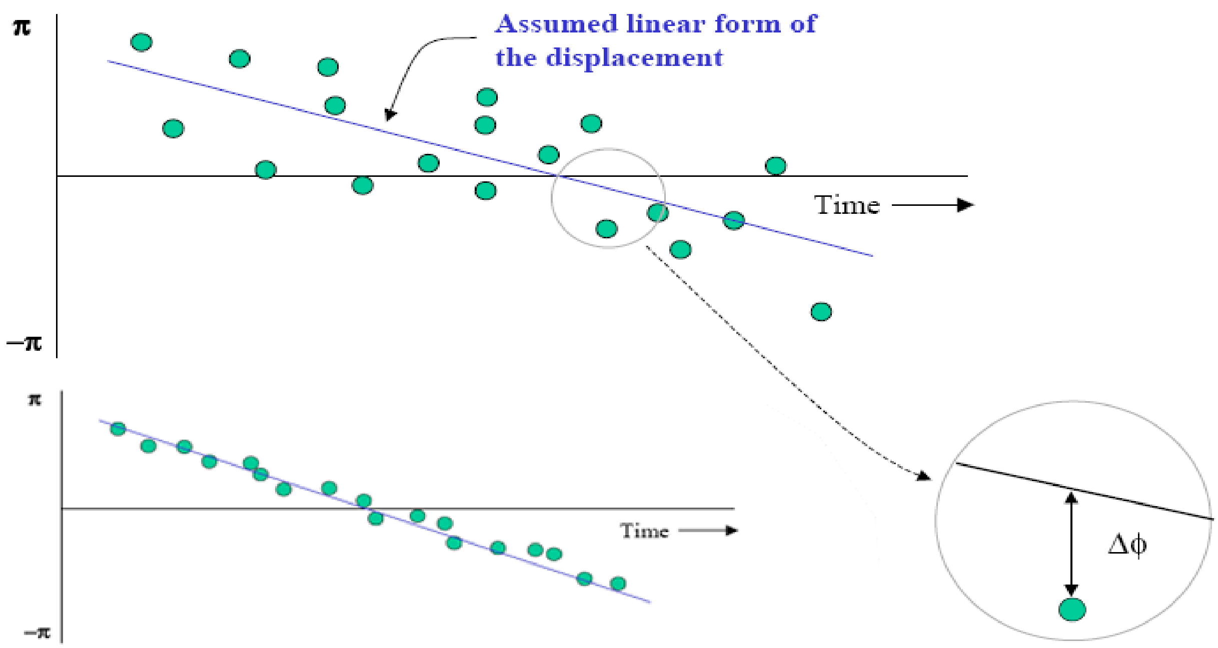

3-D phase unwrapping - Spatial unwrapping

Integrate phase difference of neighbor points in triangular network to determine absolute displacement components

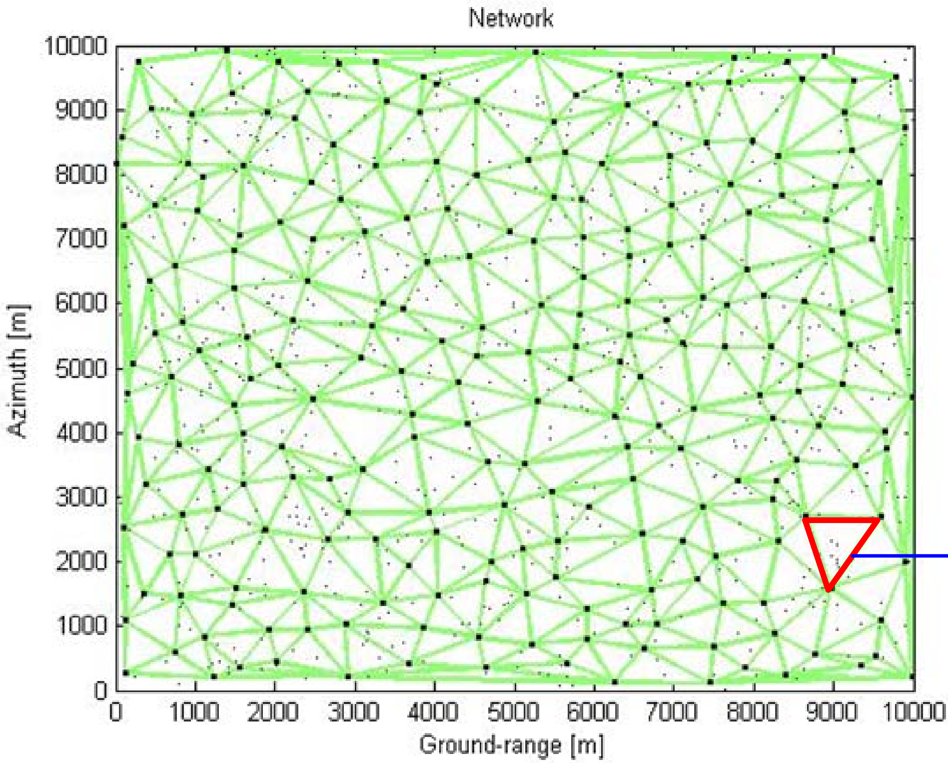

$$\min \left\| \phi_{res} \right\|^2 = \left\| \phi_{x,y} + \phi_{y,z} + \phi_{z,x} \right\|^2$$

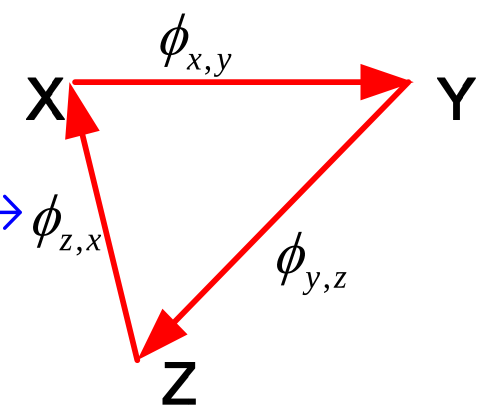

PART I

Monitoring ground subsidences with Envisat ASAR stacks in Shanghai

Experiment 1 with *Descending* data stack

9 scenes ENVISAT/ASAR images from 2003-2005

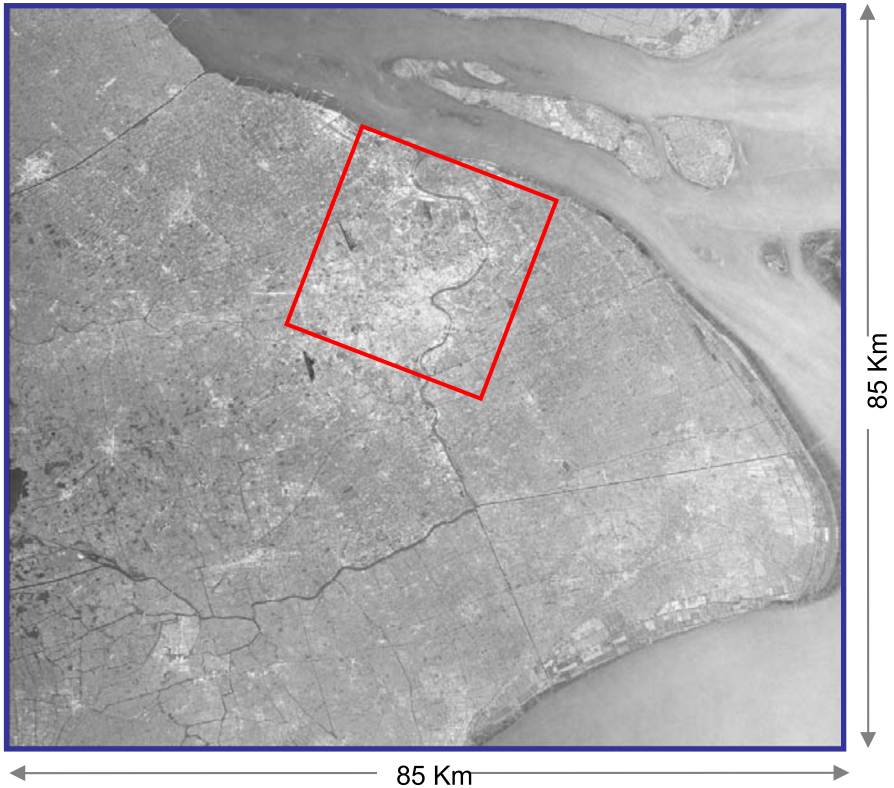

NO.	Date *(Y-M-D)*	Orbit	Doppler Frequency(Hz)
1	2003-03-25	5568	265.44653
2	2003-11-25	9075	102.01393
3	2004-05-18	11580	132.77655
4	2004-06-22	12081	380.3226
5	2004-11-09	14085	146.211
6	2004-12-14	14586	122.94549
7	2005-02-22	15588	146.7093
8	2005-03-29	16089	136.22597
9	2005-08-16	18093	156.00352

Yearly average ground subsidence on ASAR dataset from 2003-2005

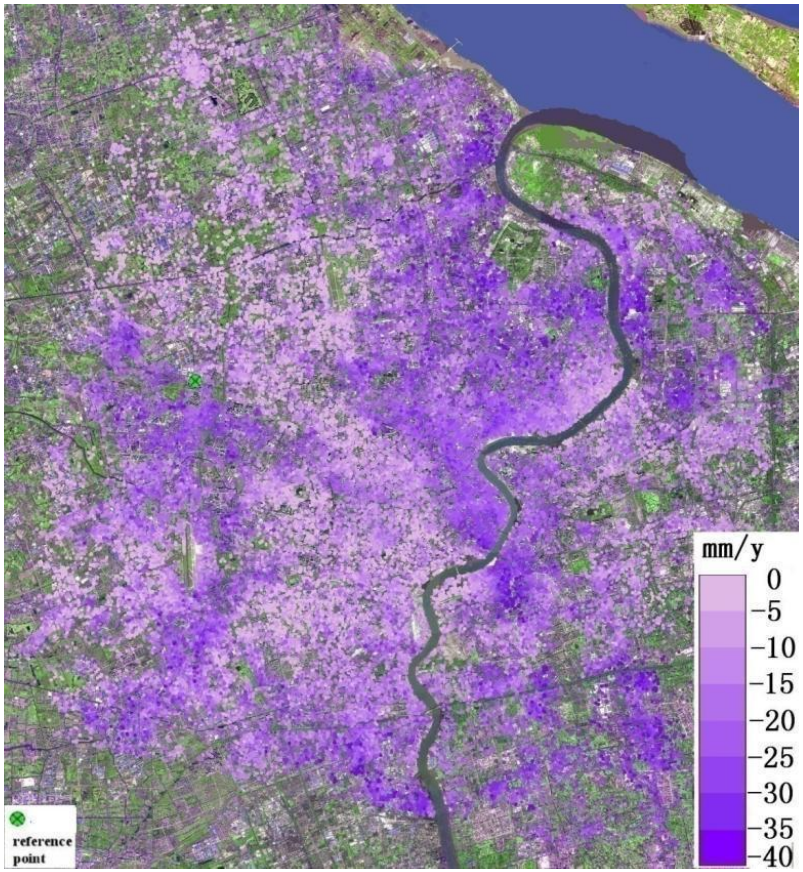

Ground subsidence contour surveyed in 2005

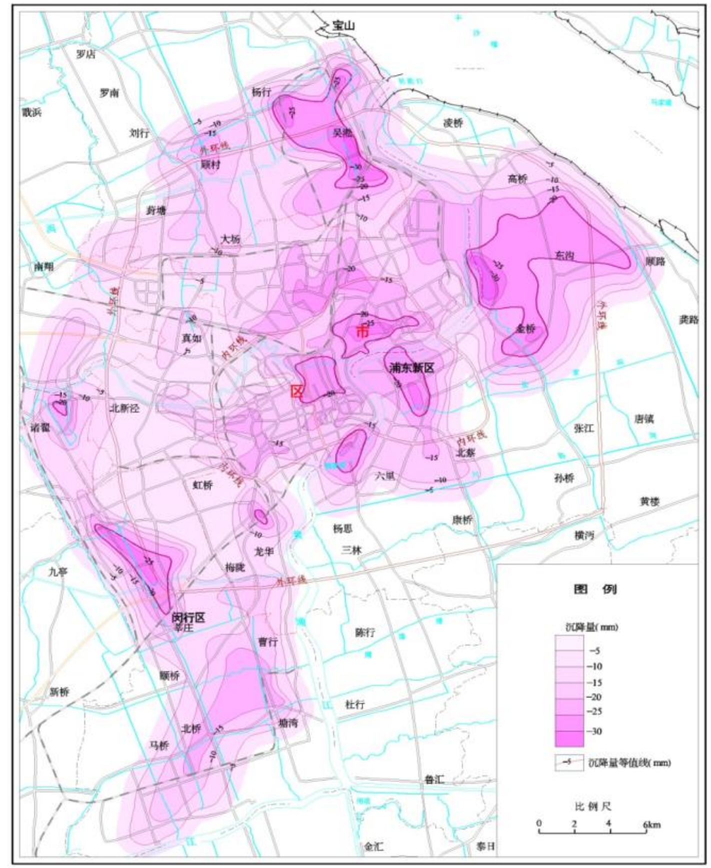

The validation of subsidence velocity

The leveling benchmark surveyed in 2003-2005

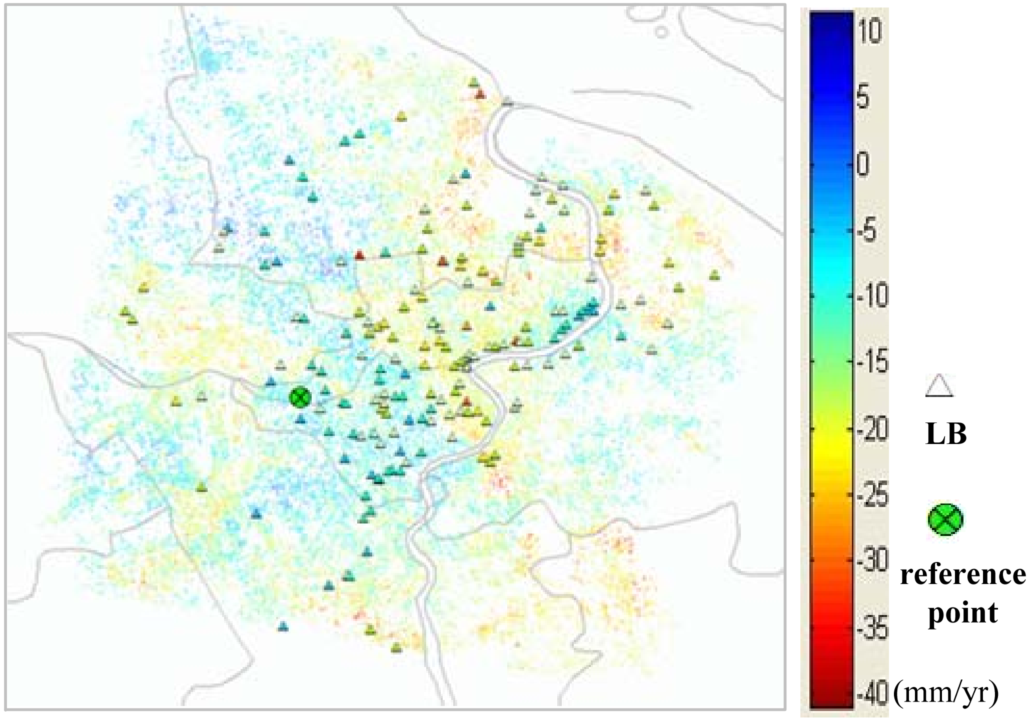

The histogram of errors distribution

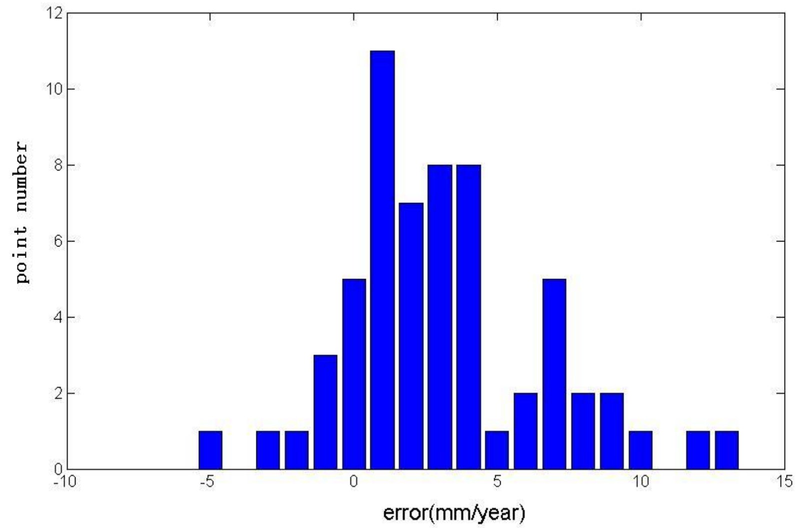

Mean : 1.08mm
STD : 4.22mm

Experiment 2 with *Ascending* data stack

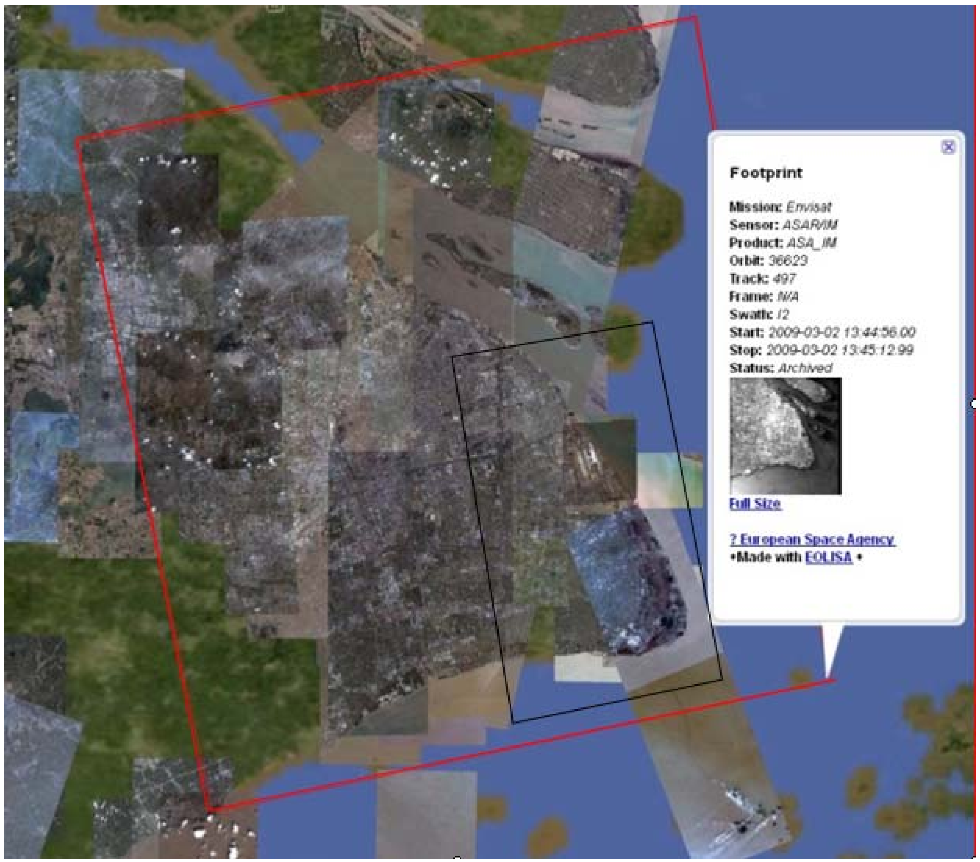

No.	Acquisition date	Perp. Baseline (m)	Temporal Baseline (days)	fDC diff (Hz)	Total correlat-ion
1	29-Oct-07	-33.11	-280	4.74	0.82
2	3-Dec-07	-96.64	-245	1.79	0.79
3	7-Jan-08	33.05	-210	2.72	0.86
4	11-Feb-08	-288.62	-175	-7.00	0.66
5	17-Mar-08	-69.62	-140	3.80	0.86
6	21-Apr-08	-272.83	-105	-5.21	0.71
7	26-May-08	17.50	-70	4.58	0.94
8	30-Jun-08	142.65	-35	-1.32	0.85
9	4-Aug-08	-- --	-- --	-- --	-- --
10	8-Sep-08	-330.72	35	-4.55	0.68
11	13-Oct-08	255.49	70	-3.61	0.74
12	17-Nov-08	-172.14	105	-2.54	0.79
13	22-Dec-08	185.80	140	-0.91	0.77
14	26-Jan-09	-214.39	175	-1.01	0.73
15	2-Mar-09	130.33	210	-5.74	0.78
16	6-Apr-09	-166.99	245	-4.47	0.73
17	11-May-09	295.92	280	-13.83	0.61
18	20-Jul-09	123.15	350	-2.71	0.72
19	24-Aug-09	-137.64	385	-11.30	0.68
20	28-Sep-09	-146.21	420	-5.02	0.67
21	2-Nov-09	117.62	455	-1.44	0.67
22	7-Dec-09	-217.21	490	-0.61	0.59
23	11-Jan-10	224.86	525	-100.45	0.53
24	15-Feb-10	-198.83	560	-7.39	0.56

Deformation velocity map of shanghai

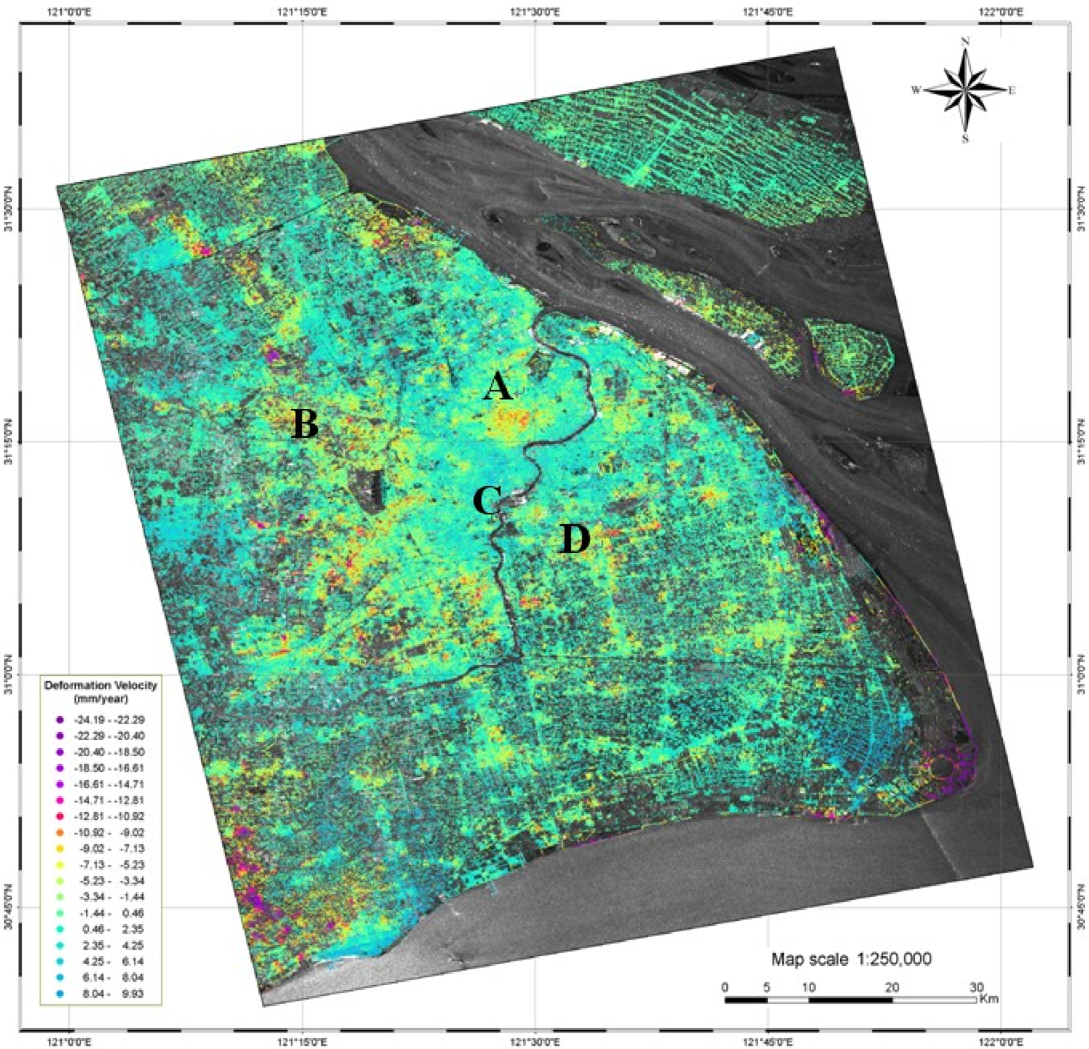

- **The subsidence velocity varies from -25mm/year to 9 mm/year**
- **zones showing obvious subsidences:**

A west of Yangpu district and east south of hongkou district；

B around hongqiao international airport；

C and D are influenced respectively by subway line 8 and World EXPO 2010 on the two sides of Huangpu river

The validation of subsidence velocity

The distribution of benchmarks

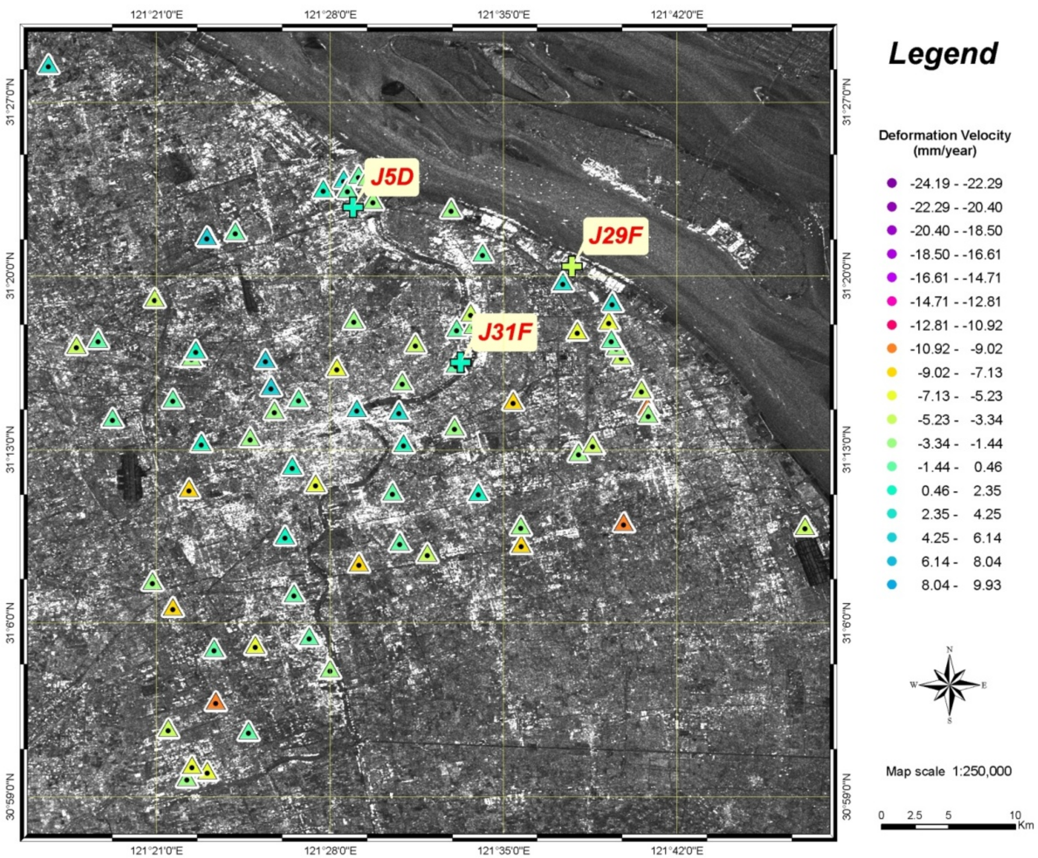

The histogram of errors distribution

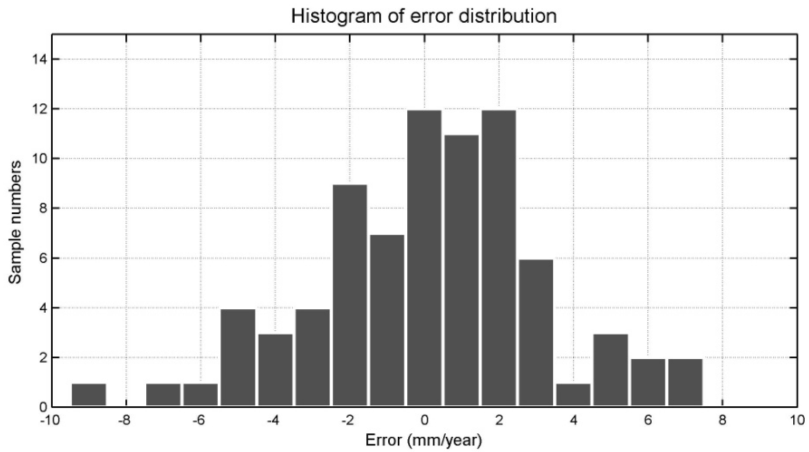

STD :3.17mm

The time series comparison between GCPs and PSs

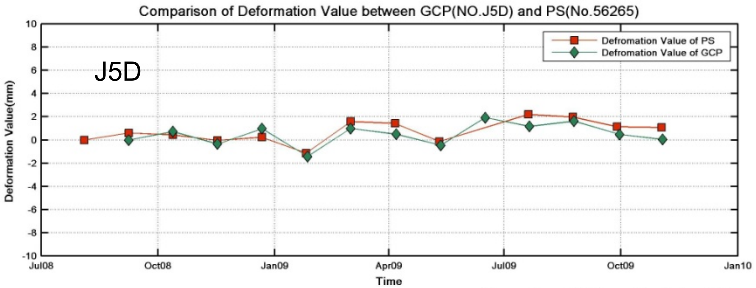

Within the minimum distance, stable point targets closest to one benchmark will be selected for comparing with subsidence values.

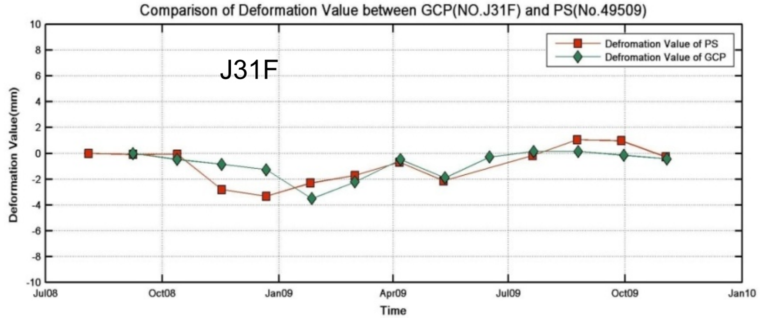

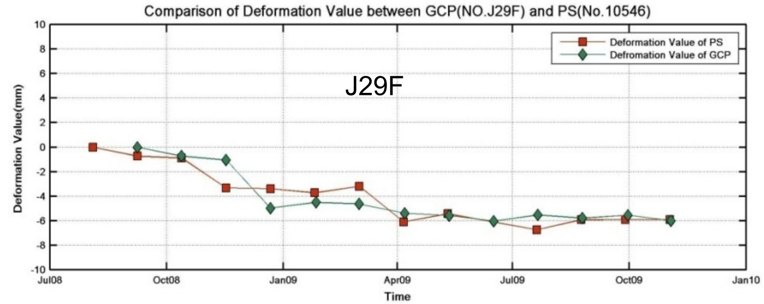

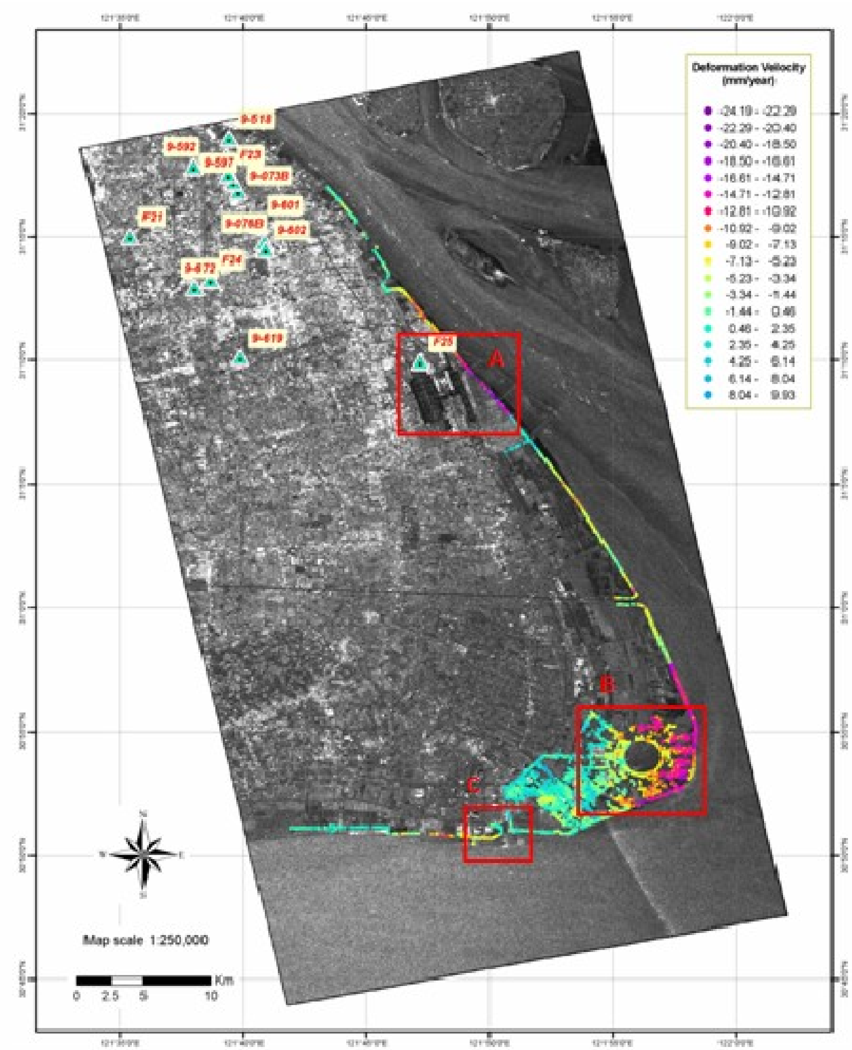

Deformation velocity map of shanghai levees

- Almost 70 km levees were monitored.
- The distribution of 14 benchmarks is shown in the left pictures.
- STD=3.07mm.
- Focus on the highlighted rectangle areas：
- A –Pudong international airport
- B – Lingang town
- C – Luchao harbor

The results and discussions of the deformation velocity

The deformation of levees is more serious than that of the airport. The levees are built on the soft soil and the ocean tide cause serious sediment deposition outside of the levee.

The soil in the east is filled recently and the compactness and uniformity is poor. This kind of less consolidated soil may result in considerable unevenly distributed ground subsidence.

The levees in the southern of Luchao harbor have experienced a serious subsidence, while the eastern slope of Luchao Harbor is generally stable. There are large areas of less filling soil consolidation in the southern slope.

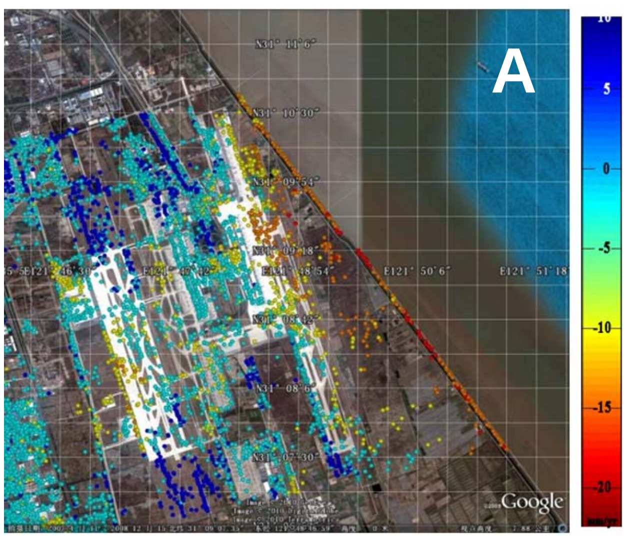

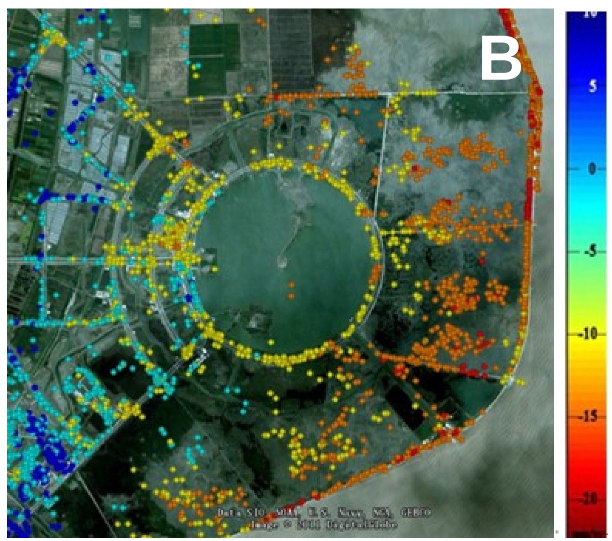

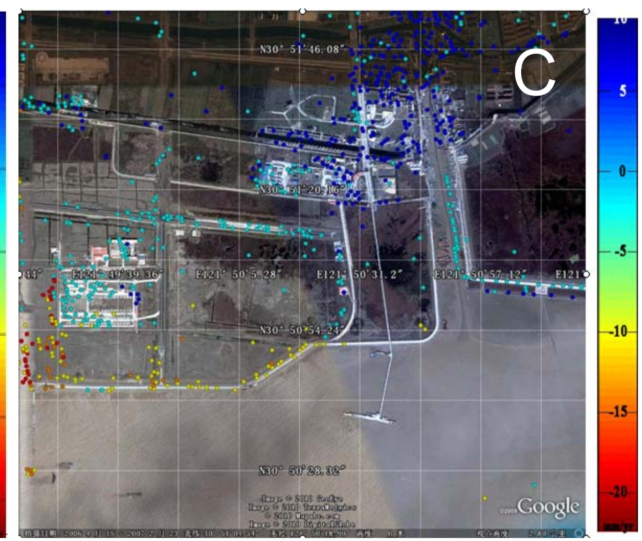

PART II

Preliminary results for monitoring subsidence with HR-SAR data stack

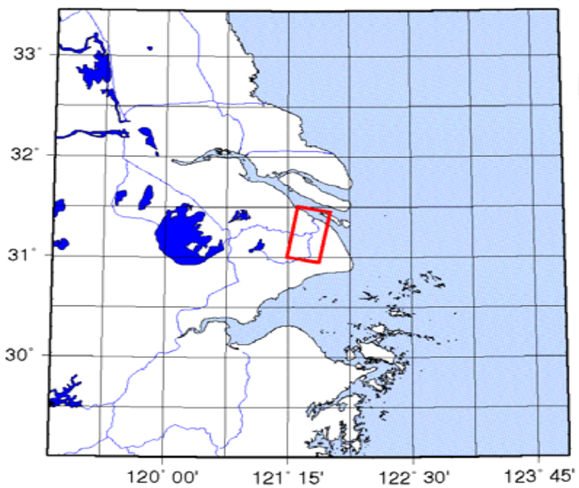

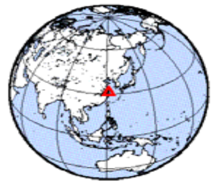

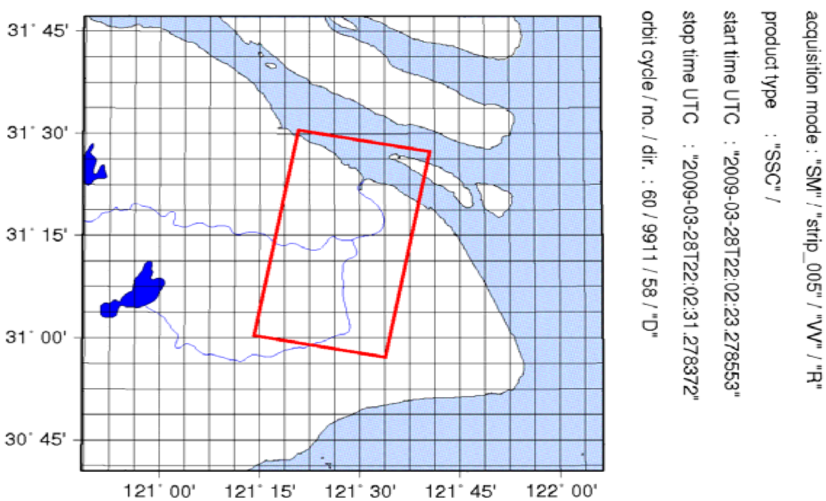

Information of TerraSAR-X Data

Mode：StripMap ；Orbit：Descending

No.	Acquisition Date	Orbit No.	No.	Acquisition Date	Orbit No.
1	2008-04-21	4734	11	2009-09-20	12583
2	2008-08-20	6571	12	2009-10-12	12917
3	2009-03-28	9911	13	2009-10-23	13084
4	2009-04-08	10078	14	2009-11-14	13418
5	2009-04-19	10245	15	2009-12-06	13752
6	2009-05-11	10579	16	2009-12-17	13919
7	2009-05-22	10746	17	2009-12-28	14084
8	2009-06-02	10913	18	2010-01-08	14253
9	2009-06-24	11247	19	2010-01-19	14420
10	2009-08-29	12249	20	2010-01-30	14587

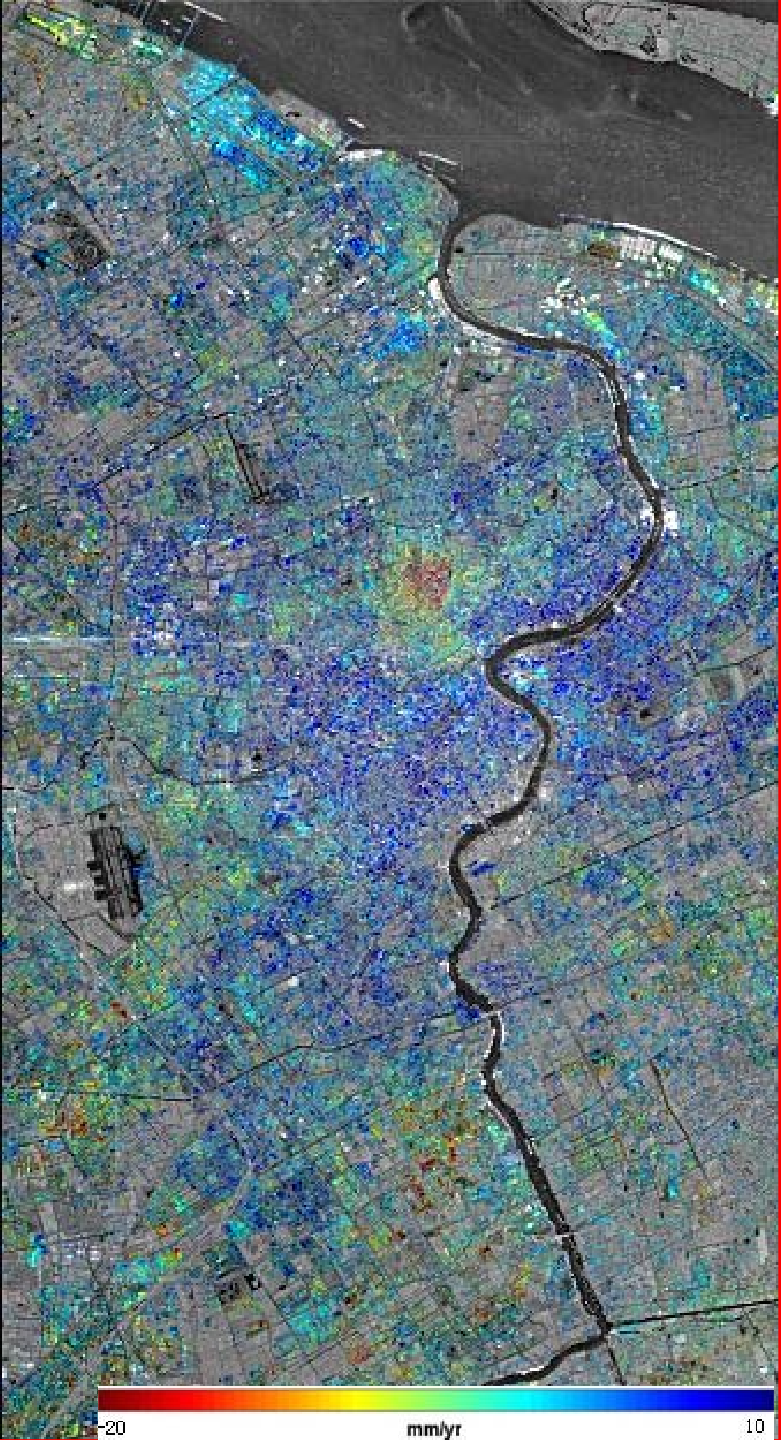

Monitoring subsidence with TerraSAR-X Data

- The subsidence velocity varies from -20mm/year to 10 mm/year;
- Coverage area: 33km×57km
- Density of coherent points = 530 ps/km^2;
- There are obvious land subsidence zones in shanghai. For example, the perimeter of the Hongkou football-court .

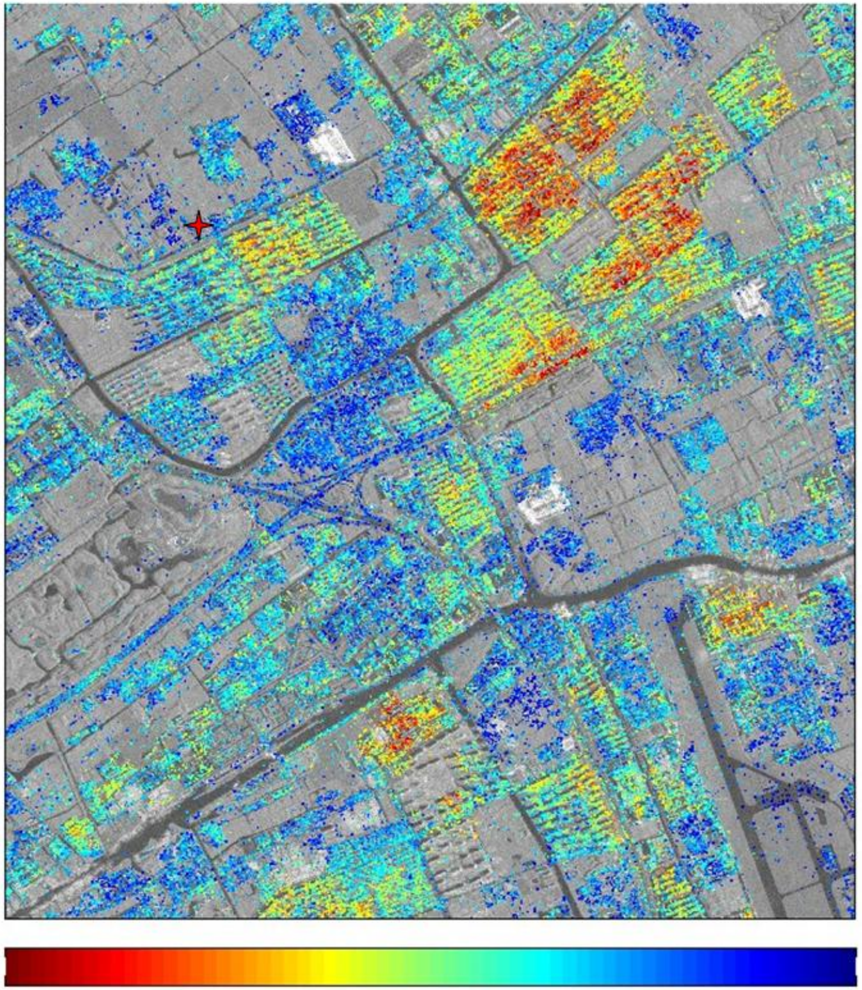

Shanghai Gucun Town

Time series analysis on leveling point：F27 (red star)

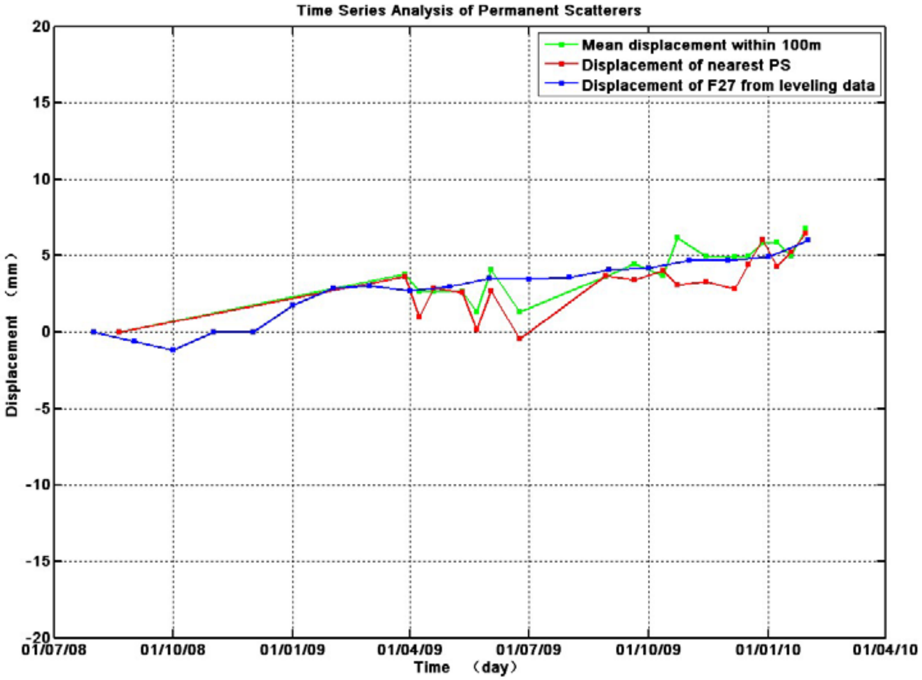

Shanghai New International Expo Center

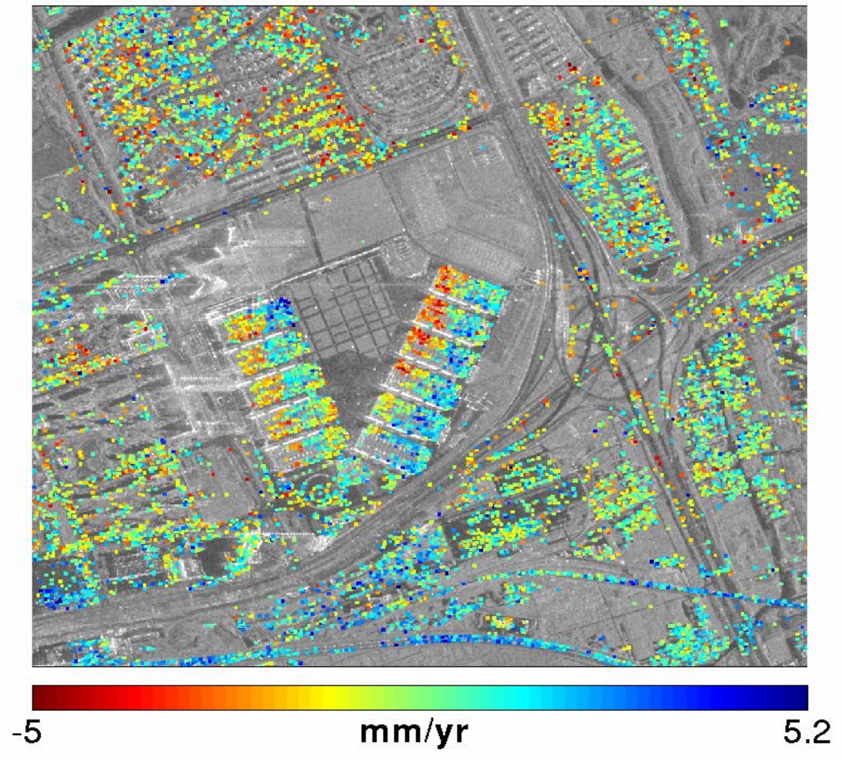

Baogang Levees

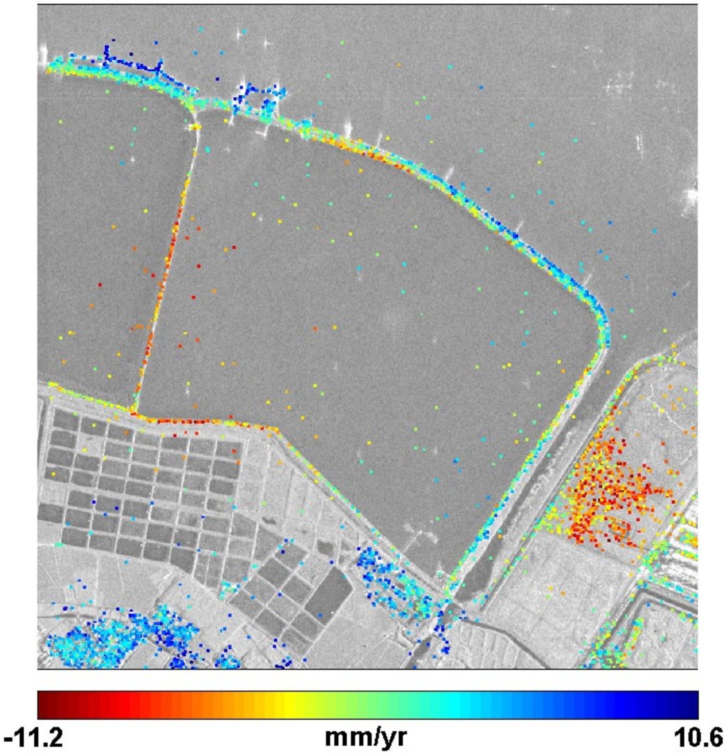

Magnetic Levitation Train Track

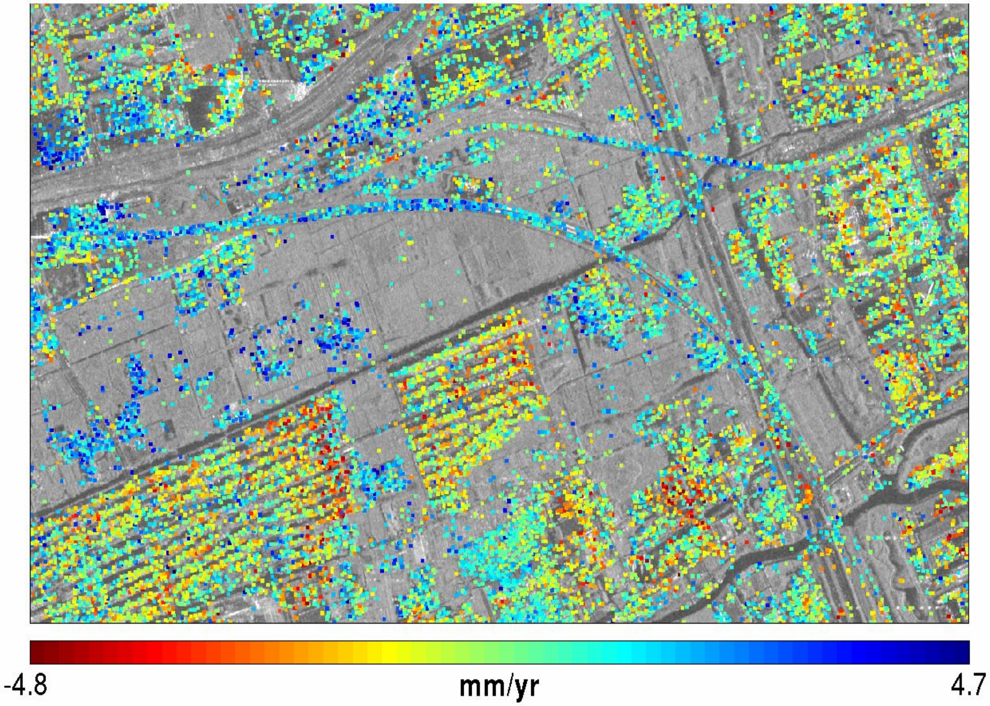

- Two Tracks:
  - urban rail transition
  - maglev train track

Shanghai subway (line 8)

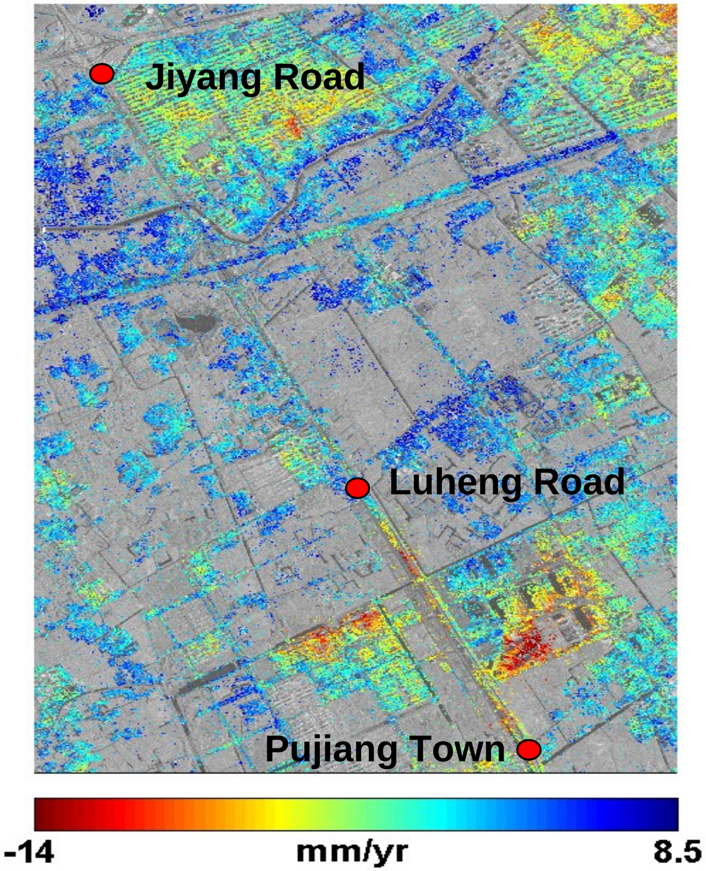

Information of COSMO-SkyMed Data

NO.	Acquisition Data (year-month-day)	Perp. baseline (m)	NO.	Acquisition Data (year-month-day)	Perp. baseline (m)	NO.	Acquisition Data (year-month-day)	Perp. baseline (m)
1	2008-12-10	-32.5	13	2009-08-15	173.9	25	2010-02-23	-411.3
2	2009-01-11	-199.3	14	2009-09-24	-370.9	26	2010-03-11	-148.7
3	2009-02-12	59.0	15	2009-10-02	-441.7	27	2010-03-19	-409.8
4	2009-02-28	552.0	16	2009-10-10	-- --	28	2010-03-27	141.2
5	2009-03-16	394.2	17	2009-10-18	247.9	29	2010-04-04	810.8
6	2009-04-01	-423.1	18	2009-10-26	401.4	30	2010-04-12	185.8
7	2009-04-09	-304.8	19	2009-11-03	404.6	31	2010-04-28	18.9
8	2009-04-17	249.3	20	2009-12-05	-322.4	32	2010-05-06	435.2
9	2009-06-04	471.9	21	2009-12-13	-148.4	33	2010-05-14	221.6
10	2009-06-12	-413.7	22	2009-12-21	104.1	34	2010-06-15	6.4
11	2009-07-14	569.3	23	2010-01-22	-281.1	35	2010-06-23	-93.2
12	2009-08-07	-193.0	24	2010-02-07	-179.8			

Preliminary results of subsidence

Shanghai New International Expo Center

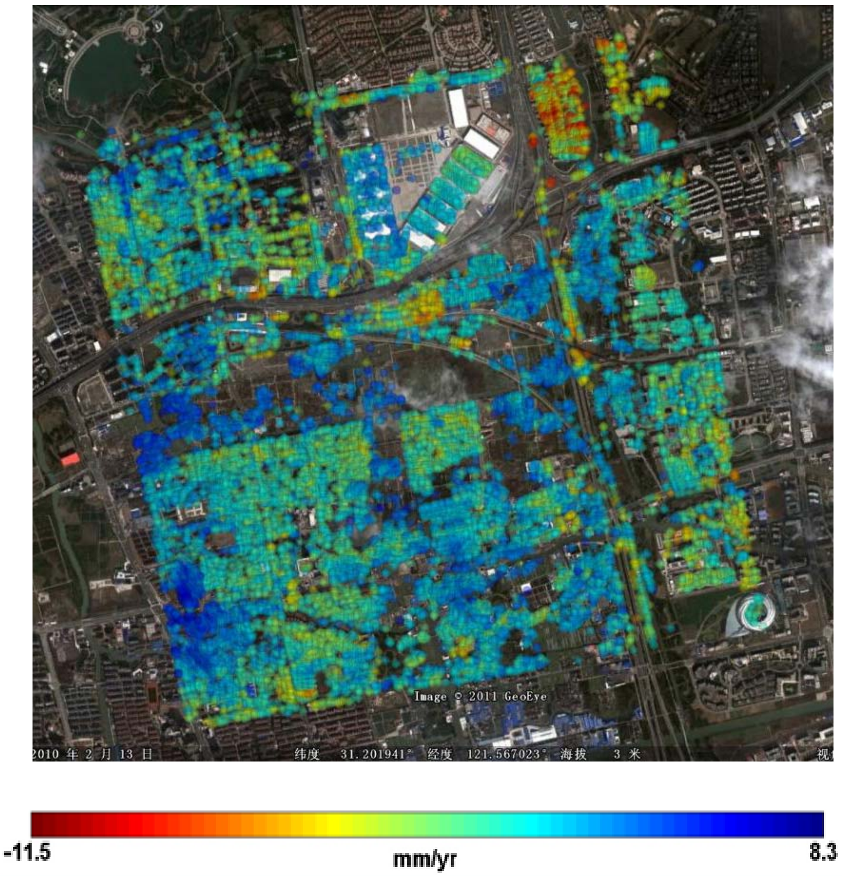

Shanghai Gucun Town

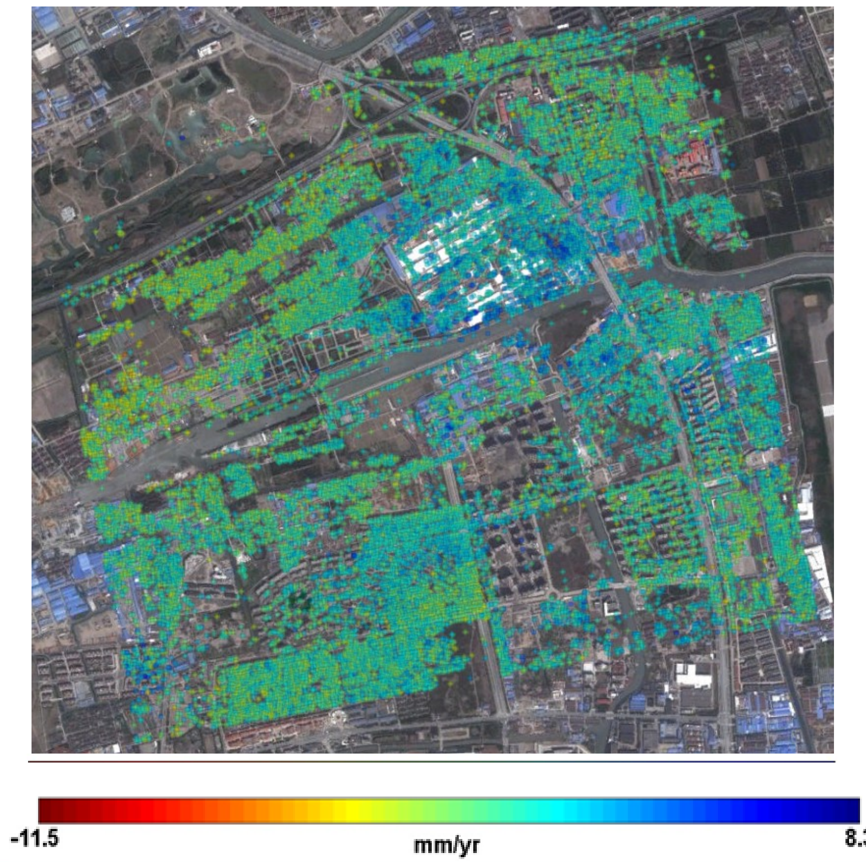

PART III

Monitoring landslide stability in Three Gorges area

Motivation for using QPS-InSAR

- Steep terrain
- Vegetation cover
- Complicated atmosphere distribution

Monitoring landslide in Three Gorges Area

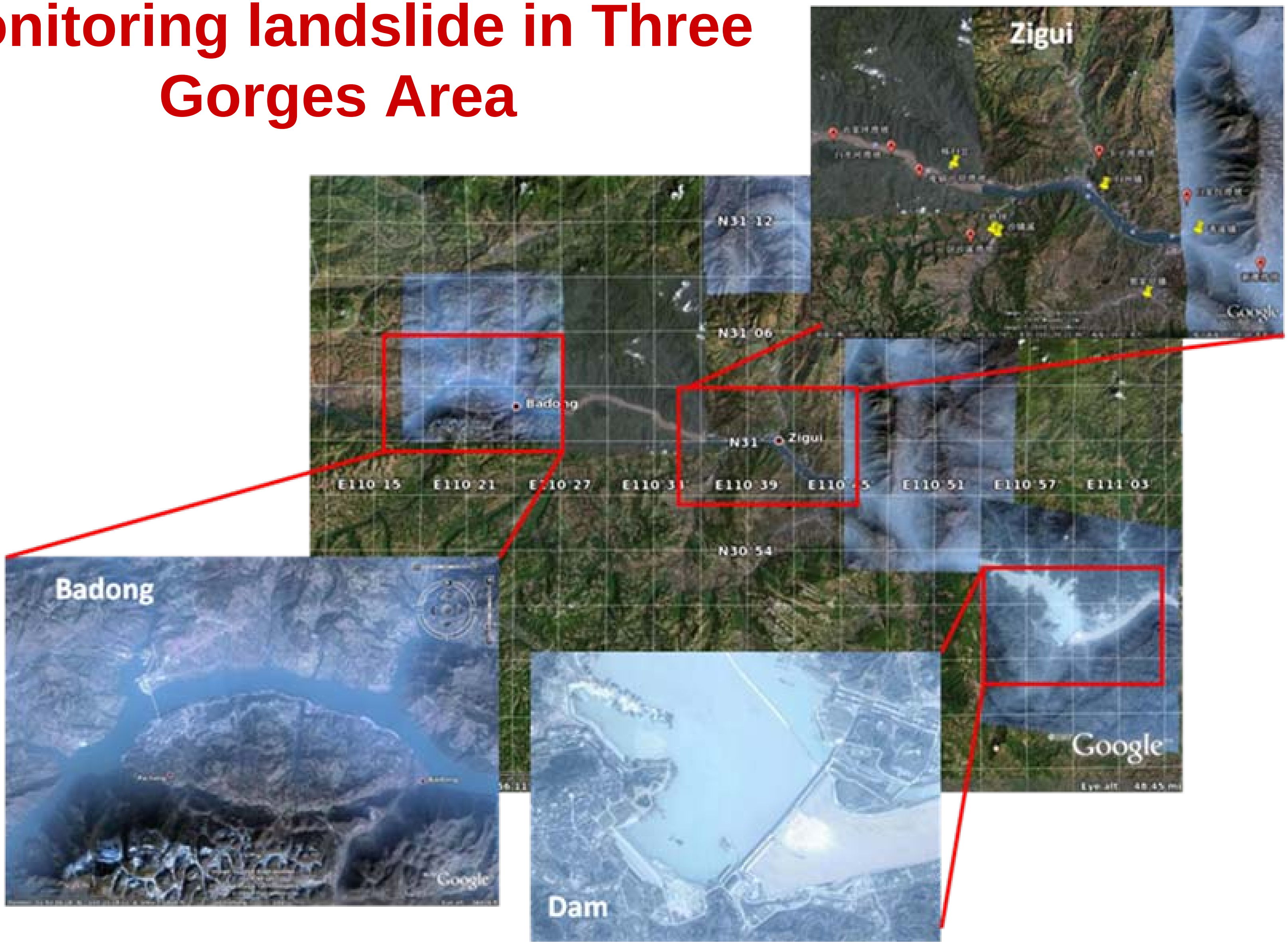

Time series InSAR analysis over Badong Town

Deformation trends from different time-series analysis methods

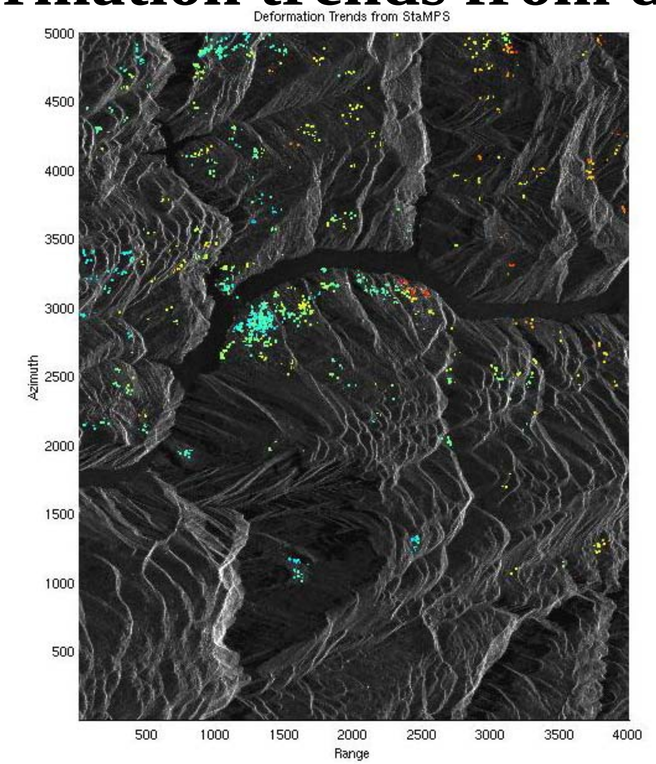

StaMPS

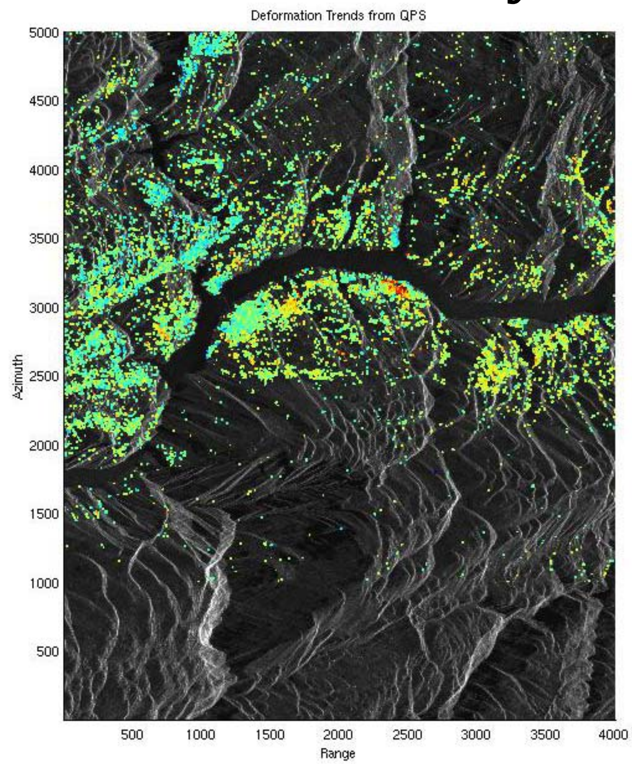

QPS

Results from ASAR data

- ➢Two subsidence areas in the south river bank of Badong city are identified.
- ➢One is in the west part of the city, about 400m above the Yangtze River.
- ➢Another area is in the east part of the city near the river.

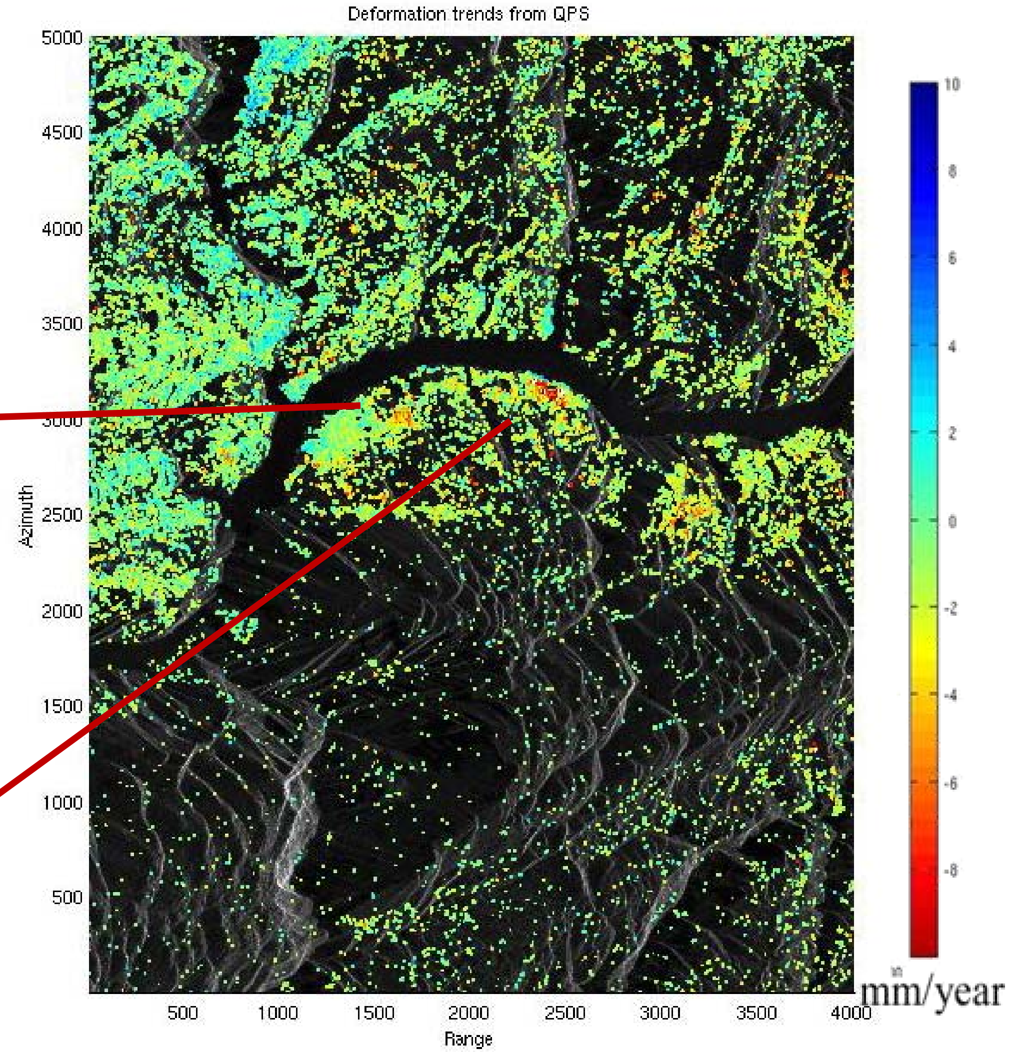

Landslides monitoring around Zigui with TerraSAR-X data

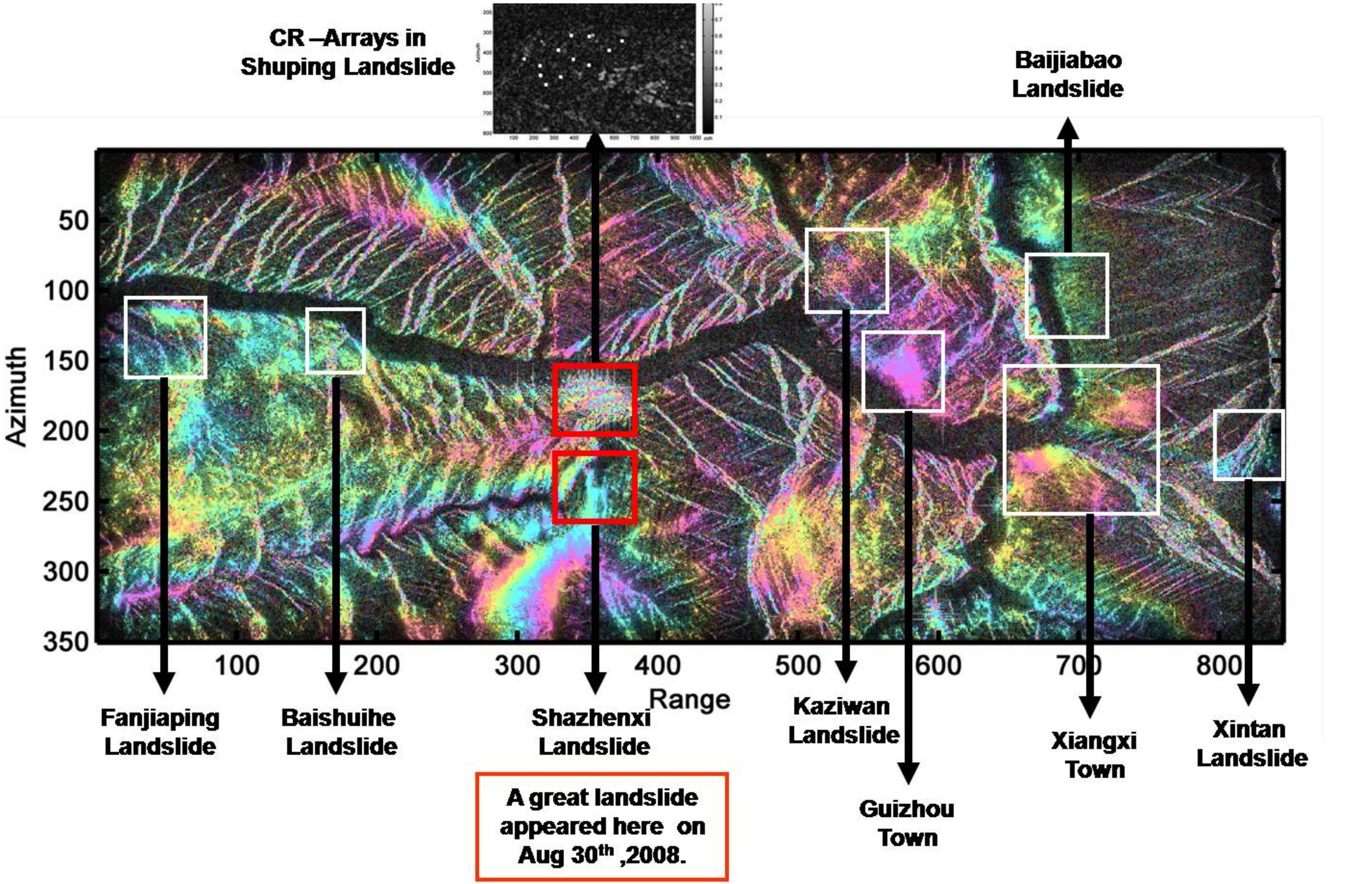

TerraSAR-X Datasets

Image Acquisiton Time	Perpendicular Baseline（m）	Water Level (m）
07-21-2008	94.7	145.1
08-12-2008	462.7	145.9
08-23-2008	62.7	145.82
09-03-2008	-200.1	145.83
09-14-2008	-20.7	145.83
10-17-2008	0	155.03
11-19-2008	-112.051	171.82
11-30-2008	160.5773	170.63
12-11-2008	255.2388	169.54
01-02-2009	11.69447	169.14
01-24-2009	40.78051	169.21
02-15-2009	-145.21	167.7
03-09-2009	204.0509	162.85
03-20-2009	-23.6477	161.72
04-22-2009	9.648303	161.07
05-14-2009	-45.7315	155.58
06-05-2009	106.82	147.47
07-08-2009	24.32009	145.59
08-10-2009	228.6826	150.91
09-12-2009	71.40709	145.29
10-04-2009	21.51874	160.7
11-06-2009	92.42501	170.87

DInSAR before the landslide (07-21-2008, 08-23-2008)

A great landslide in Shazhenxi Town appeared on Aug 30th ,2008.

DInSAR after the landslide (09-14-2008, 10-17-2008)

Differential Phase before the Landslide

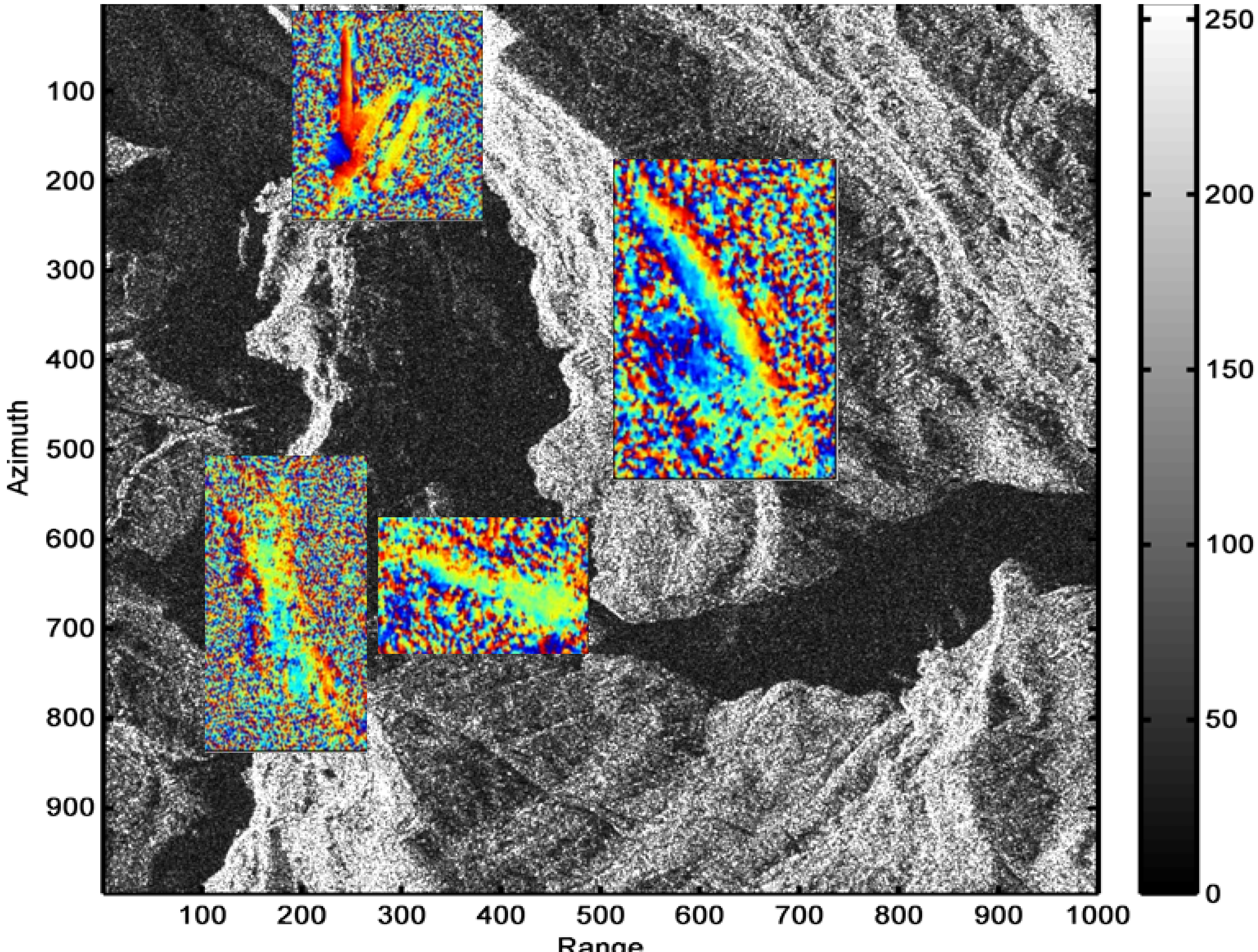

Differential Phase after the Landslide

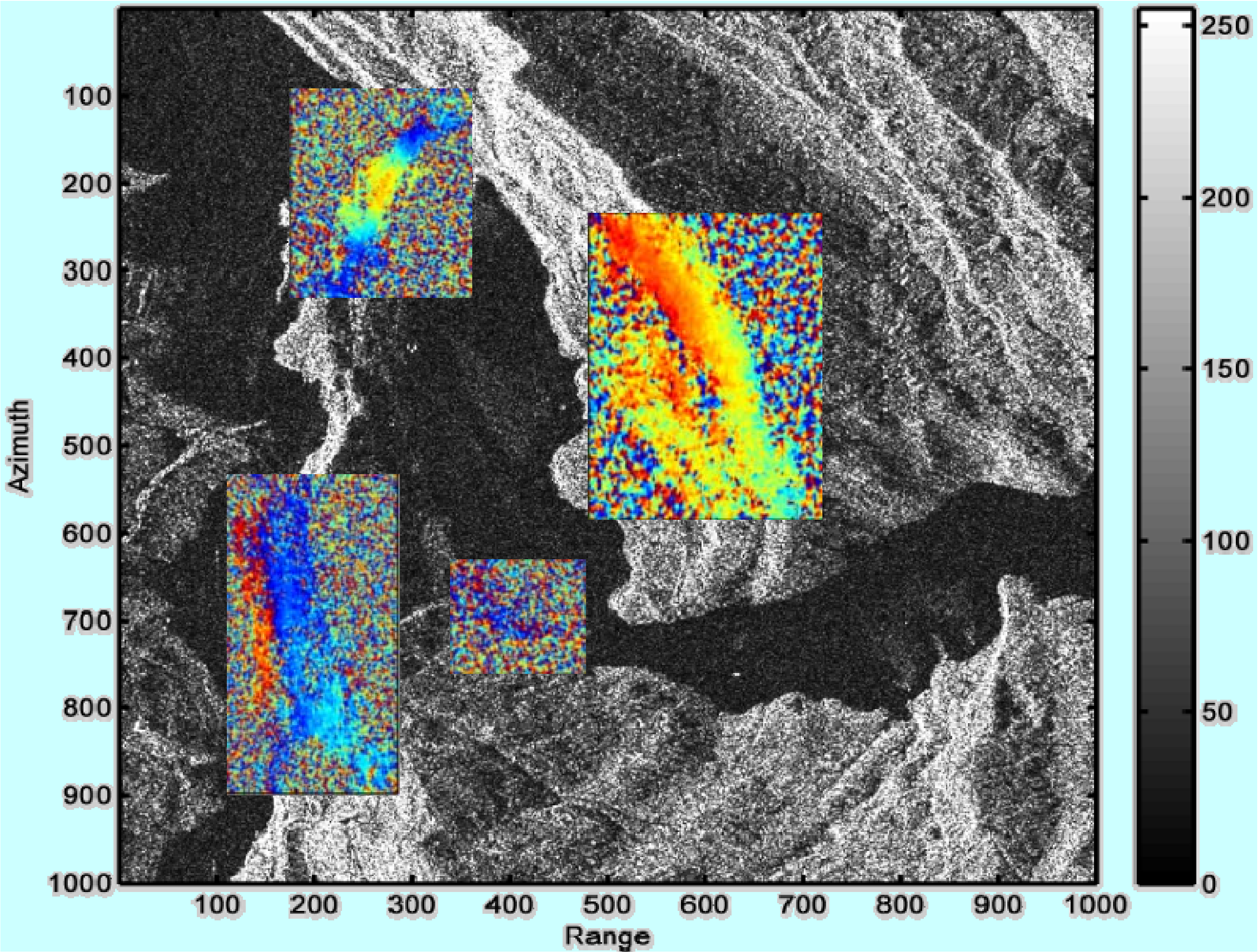

Time Series InSAR Analysis

(a) the happened landslide;
(b) and (c) are moving landslide bodies.

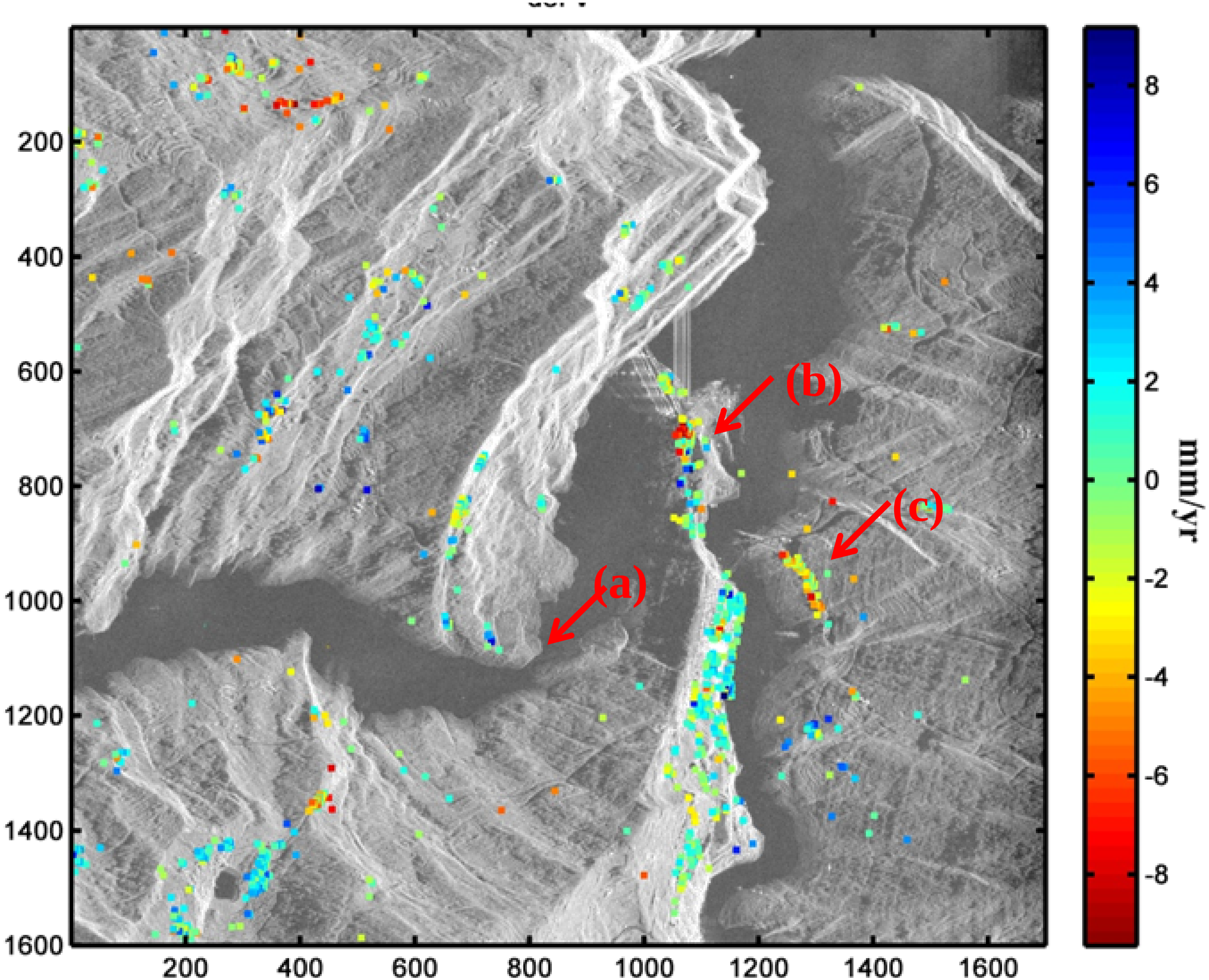

Thanks to the high resolution TerraSAR-X data, near the Shazhenxi town in this area, one landslide happened in the end of August 2008 can be identified. As reported by the official media, the heavy rain caused the landslide.

Landslide Monitoring Around ShuPing Town

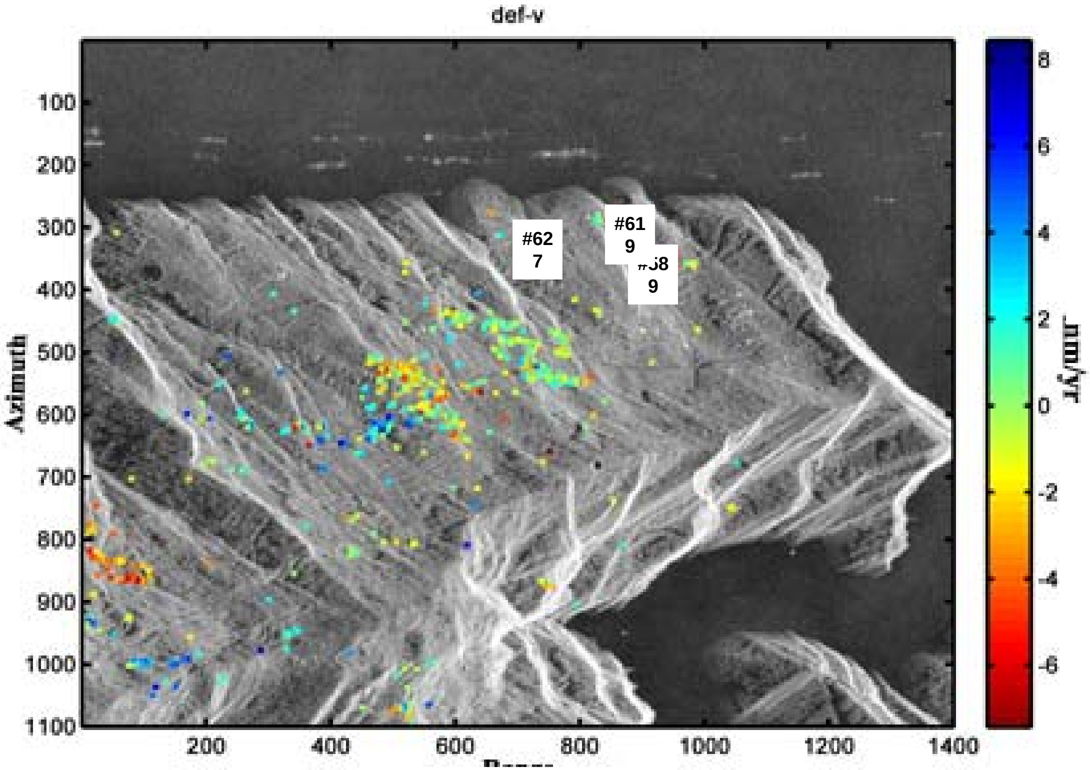

(a)

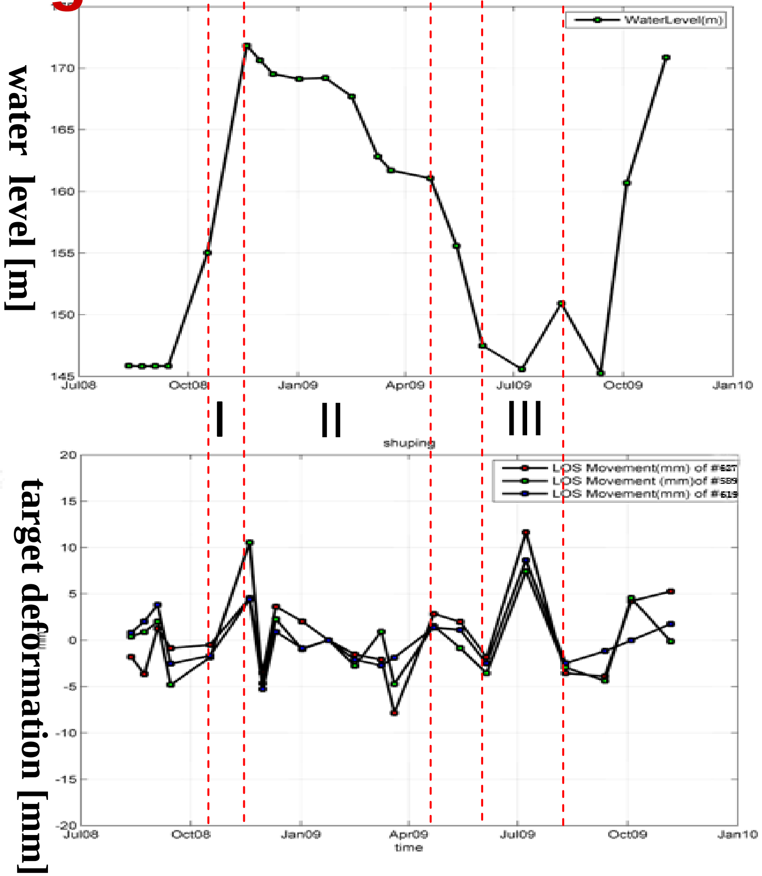

(b)

- **Period I, the rapidly changed water level caused obvious deformation.**
- **Period II, the deformation became smooth with stable water level.**
- **Period III, the scouring force from the decreasing water reduced the river bank uplifting pressure, thus significant deformation can be observed**

Experiment of ALOS/PALSAR data

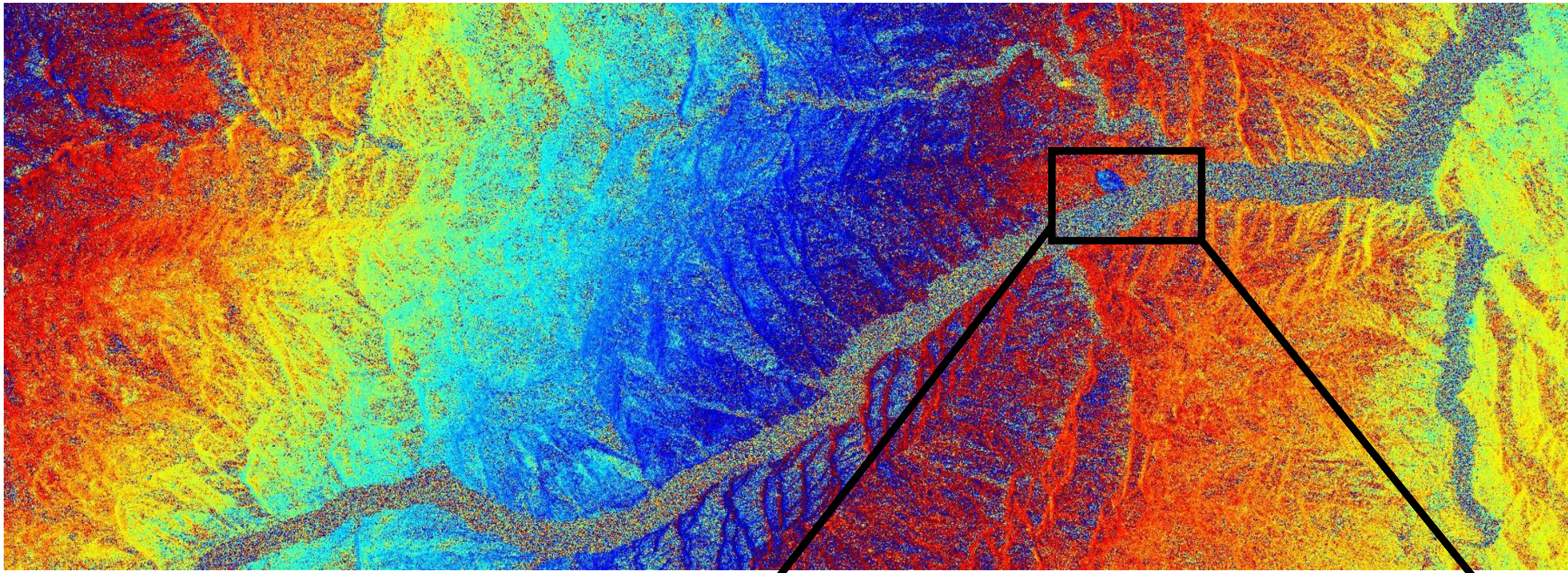

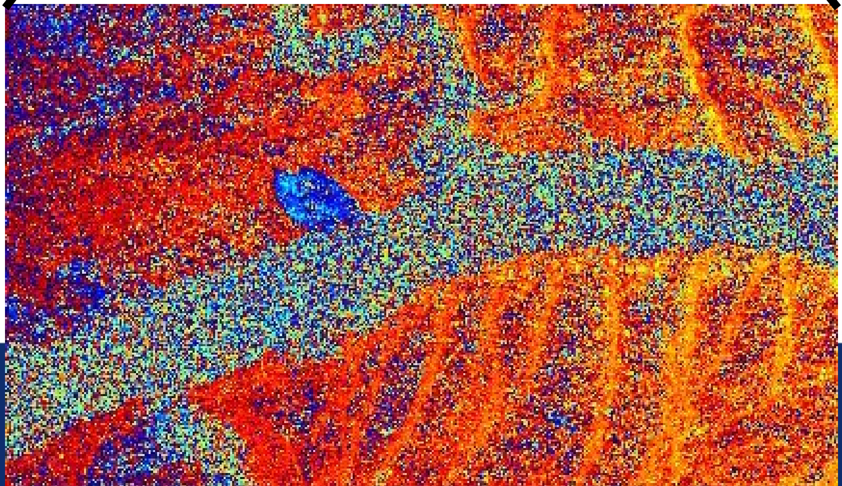

D-inteferogram from ALOS/PALSAR data

02192010/ 04062010
$B_\perp$ 192m

PART IV

DEM extraction from InSAR data

DEM construction from repeat-pass InSAR data

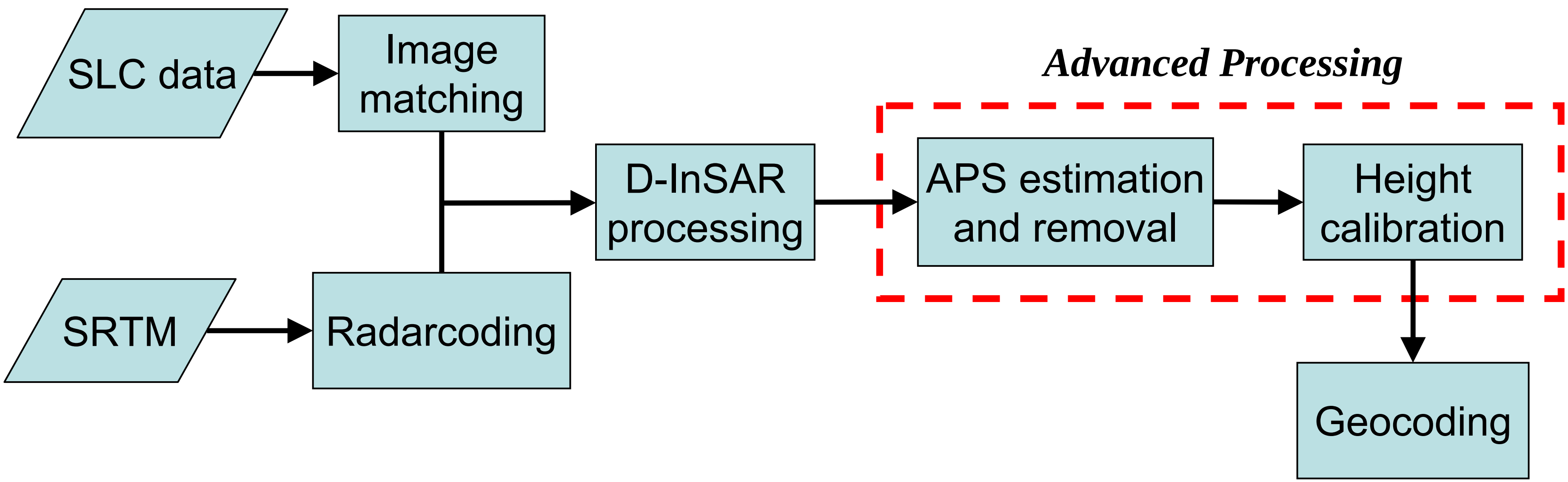

- **In repeat-pass InSAR, the atmospheric effects introduce significant errors as high as tens of meters.**
- **The height errors due to atmospheric effects are estimated from an differential interferogram, provided that deformation signals are negligible.**

DEM construction from L-band ALOS/PALSAR data

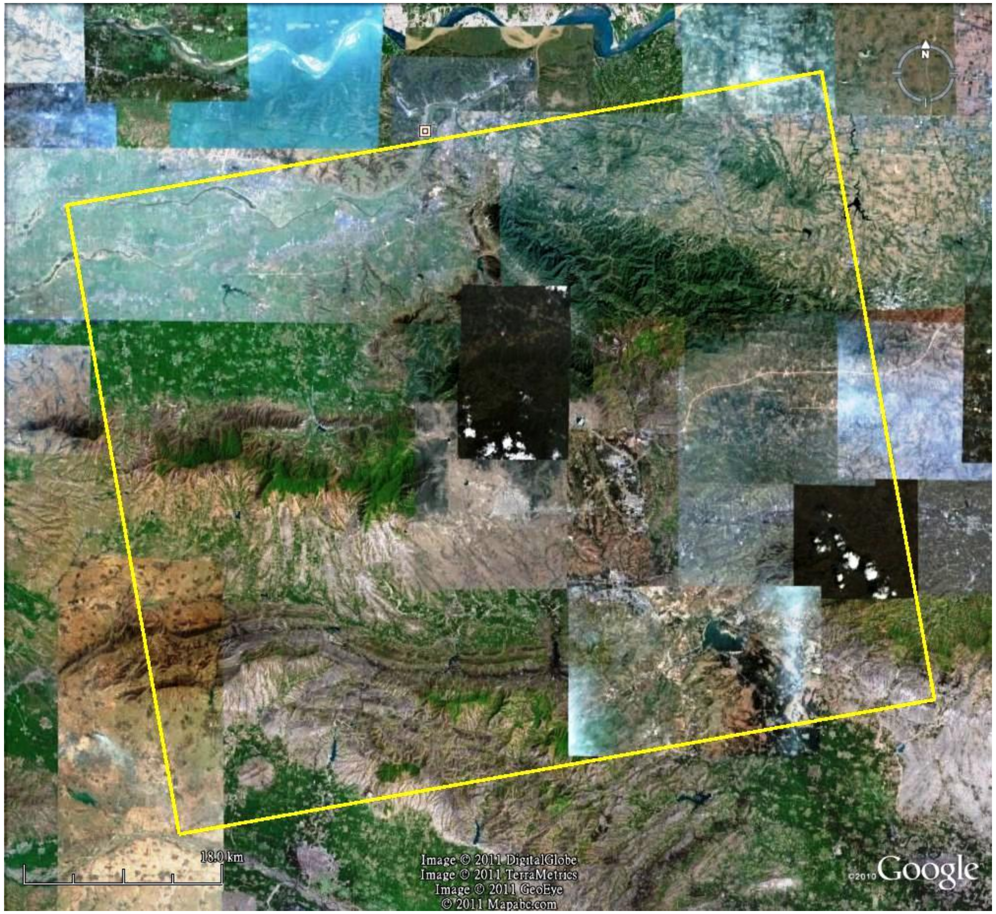

- A region about 60 km× 70 km over Mt. Song, located in Henan province of China.
- The elevation of the test site varies from 0 m to 1500 m, offering a large relief diversity for the experiment.

PALSAR interferogram parameters

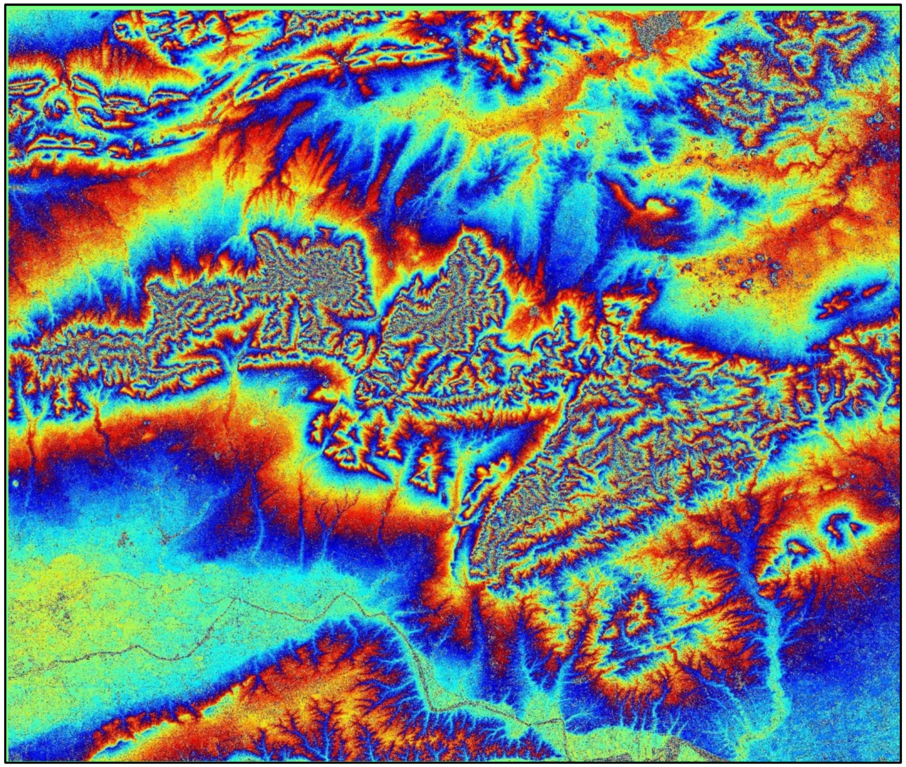

ALOS/PALSAR	
Acquisition date	2009-Nov-09 2009-Dec-25
Temporal baseline	46 days
Perp. baseline	510 m
Incidence angle	34.3°
Height ambiguity	113 m
Orbit direction	Ascending

Estimation of APS by low-pass filtering

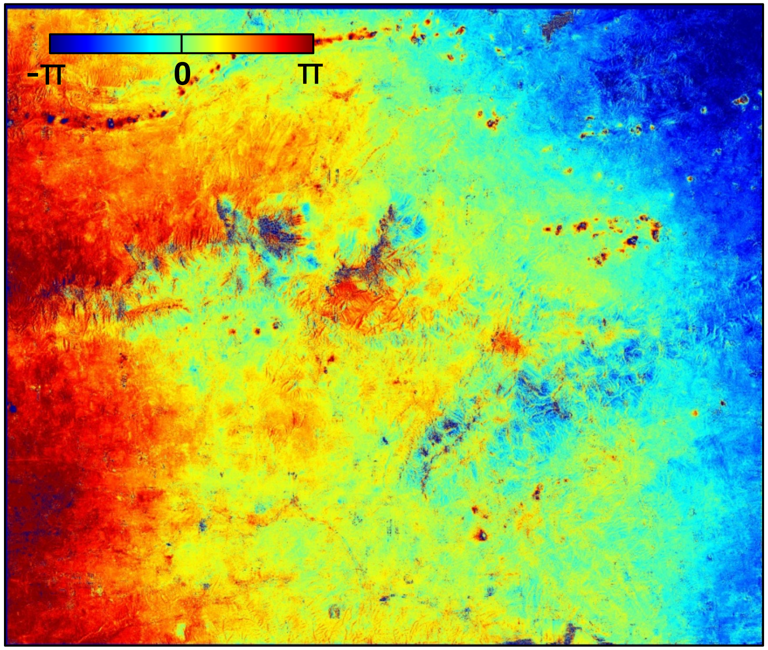

PALSAR differential interferogram

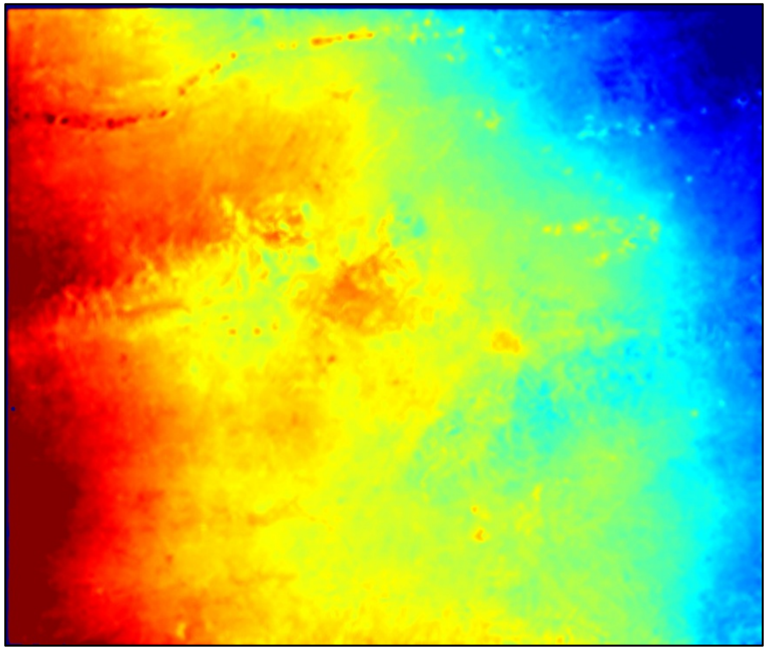

Estimated APS

PALSAR InSAR DEM and validation

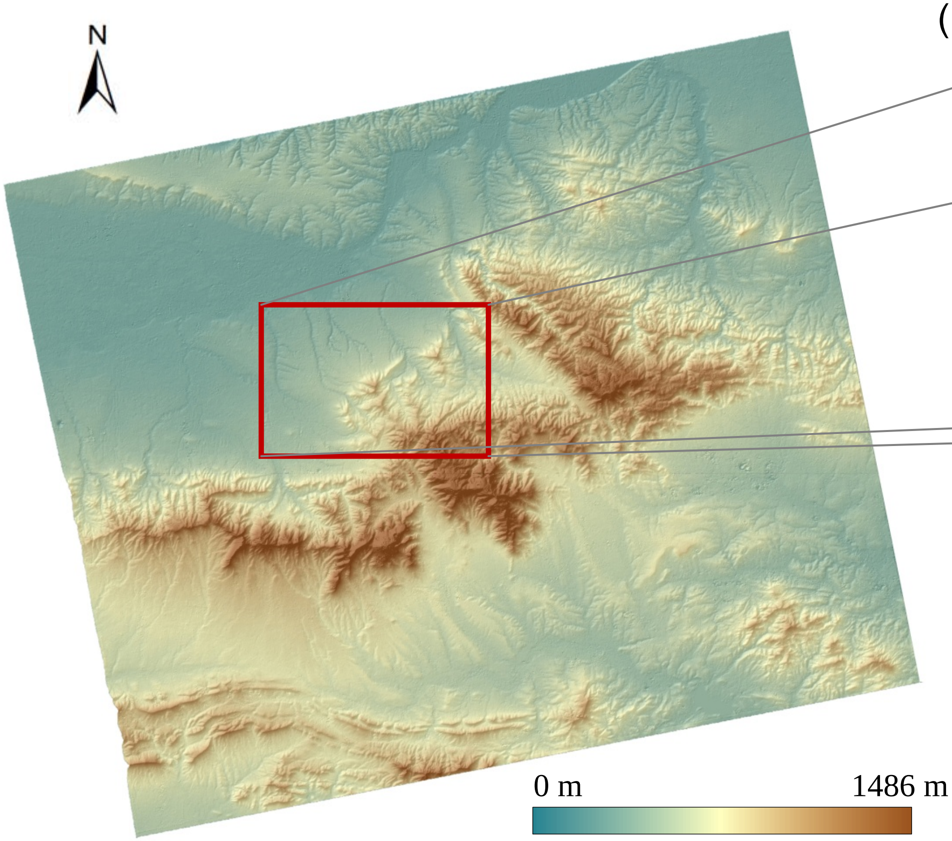

Height difference map

(PALSAR DEM vs. aerial photogrammetry 1 m DEM)

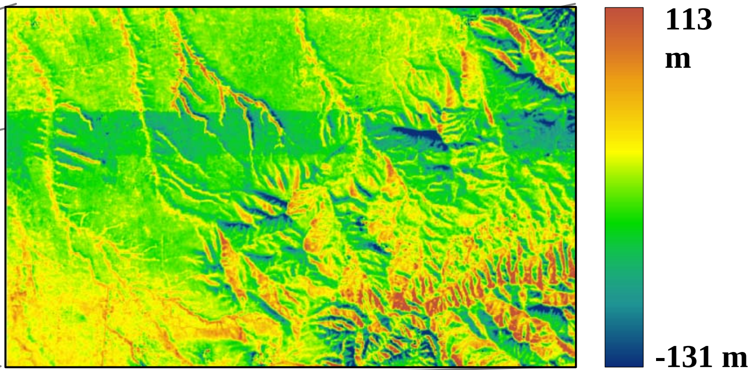

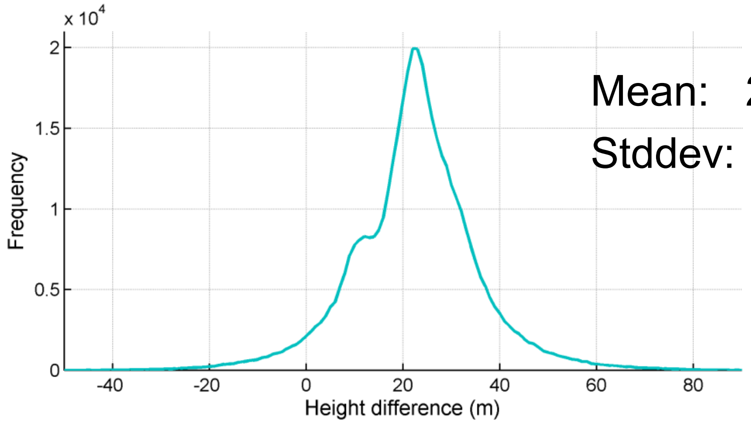

Mean: 23 m

Stddev: 13 m

DEM extraction from X-band CSKS and TSX data

- **The APS is distinguished into two types:**
  - **Stratified APS, caused by vertical stratification of atmosphere refractivity.**
  - **Turbulent APS, caused by turbulent process in the atmosphere.**

- **The stratified APS is correlated with topography:**

$$\varphi = \alpha \cdot height + \beta$$

  - **Linear model can describe the correlation between stratified APS and topography.**

- **The turbulent APS affects both mountain and flat terrain:**

$$P_N(k) = C \cdot k^{-\beta}, \quad k: \ wavenumber$$

  - **Kolmogorov's theory of turbulence can describe the turbulent APS. The Kriging interpolation based on spatial statistics is used to estimate this component.**

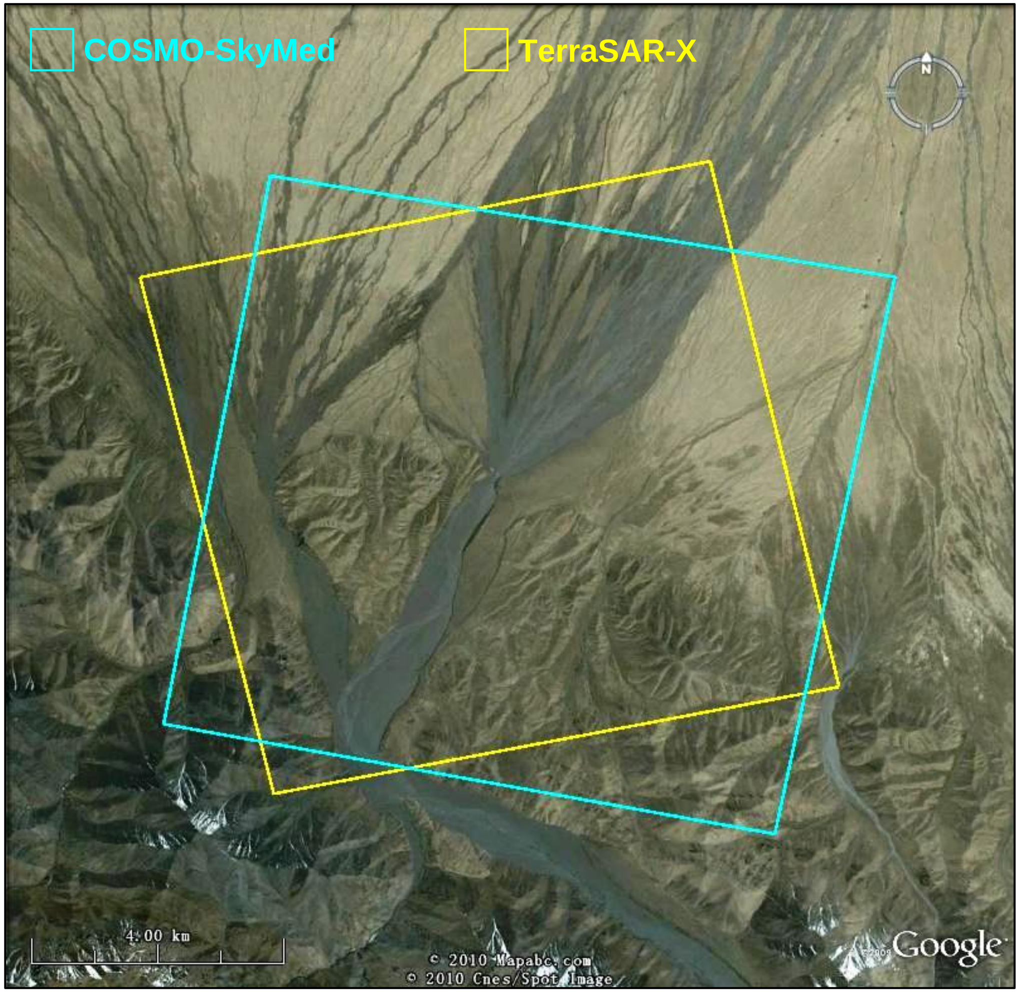

Experimental Area

- A region about 10 km× 10 km in the Mt. Qilian, located in north-western China.
- The elevation in this region varies from 3100 m to 4300 m, offering a large relief diversity for the experiment.

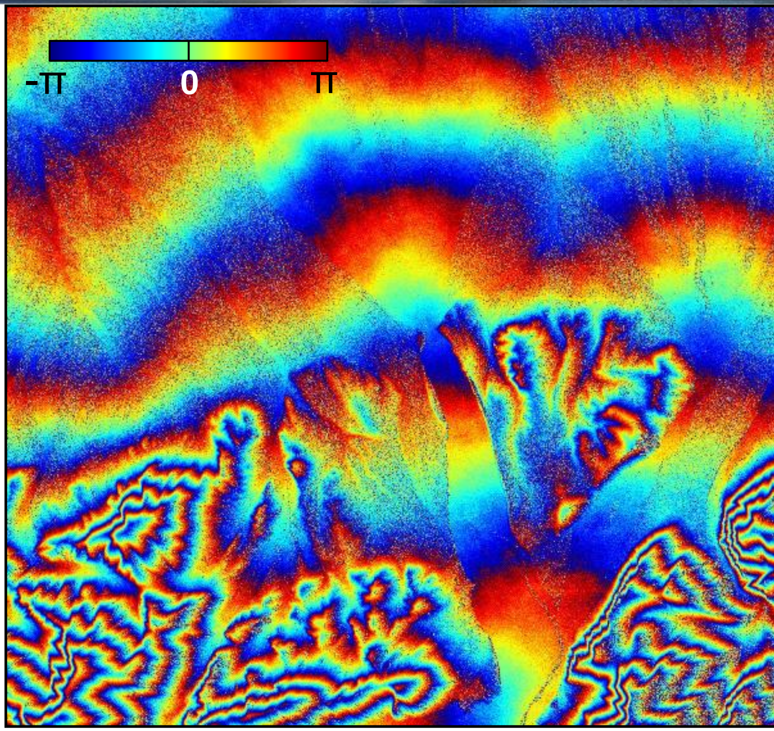

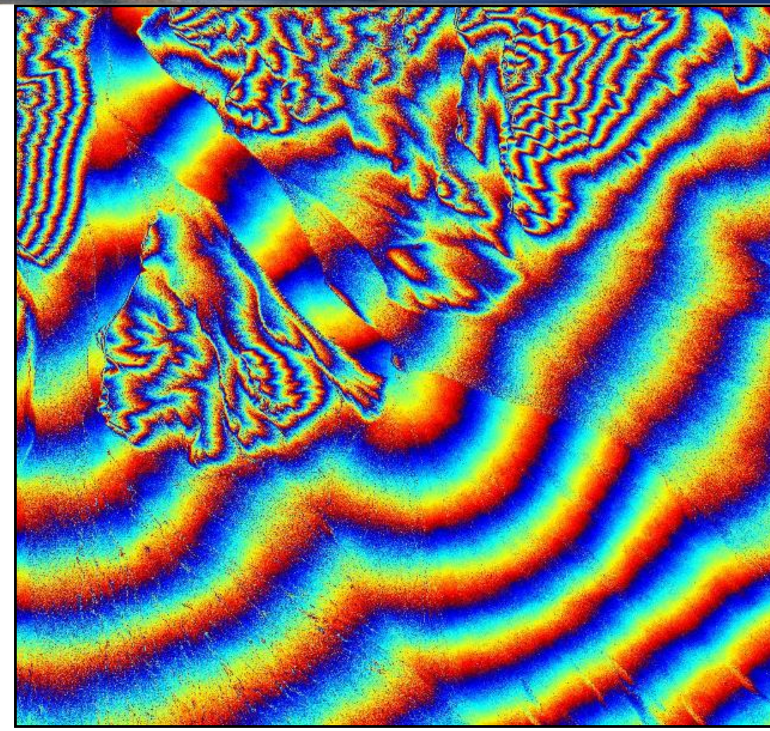

COSMO-SkyMed		TerraSAR-X
2009-Jun-03/2009-Jun-04	Acquisition date	2008-Apr-18/2008-Apr-29
63m	Perp. baseline	71m
164m	Height ambiguity	59m
48°	Incidence angle	28°
Descending	Orbit direction	Ascending

Estimation of stratified APS

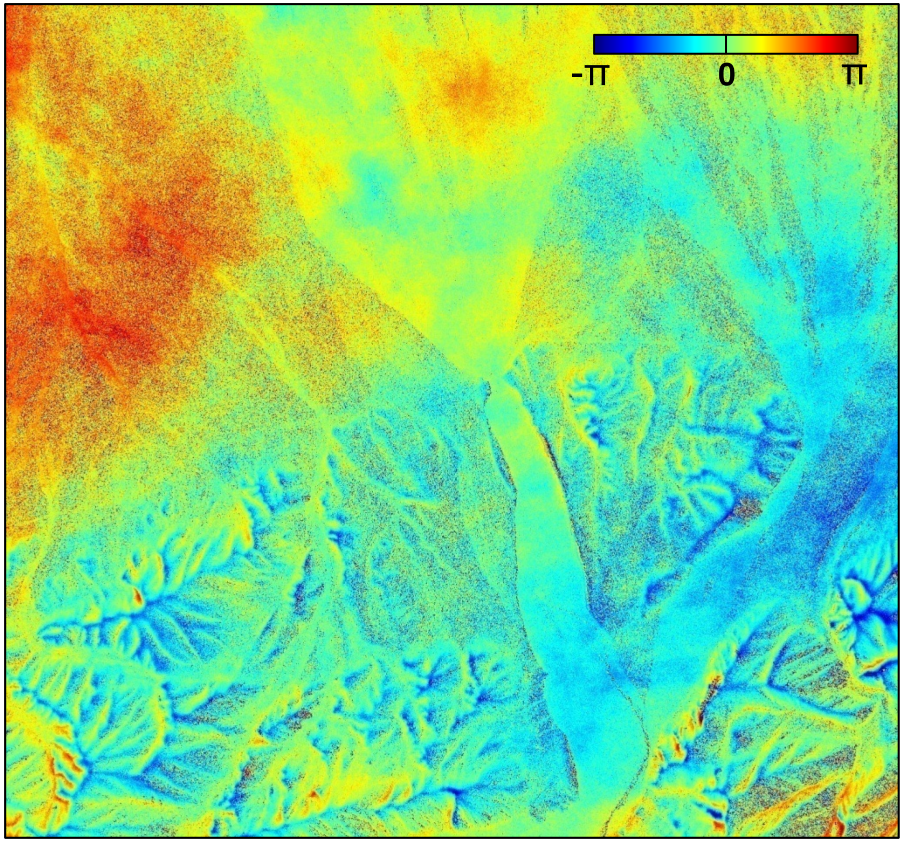

COSMO-SkyMed differential interferogram

$$\varphi = -0.010094h + 1.280681$$

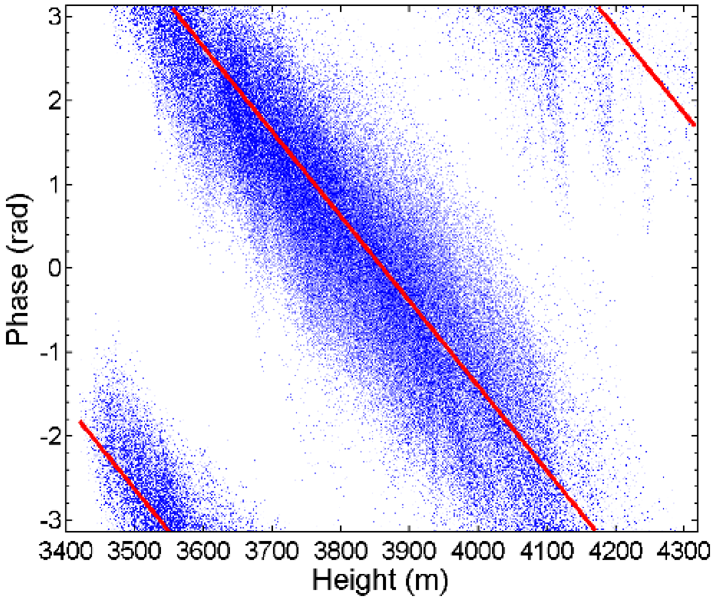

- **The differential phase is highly correlated with topography.**

Estimation of stratified APS

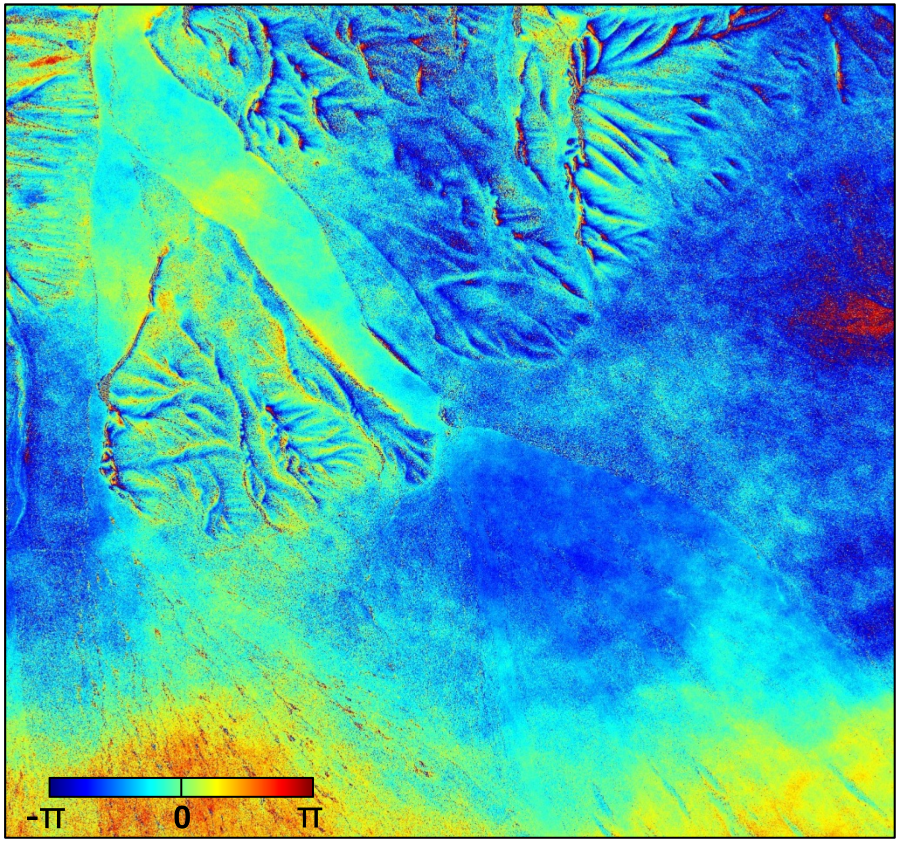

TerraSAR-X differential interferogram

$$\varphi = -0.002708h + 2.073849$$

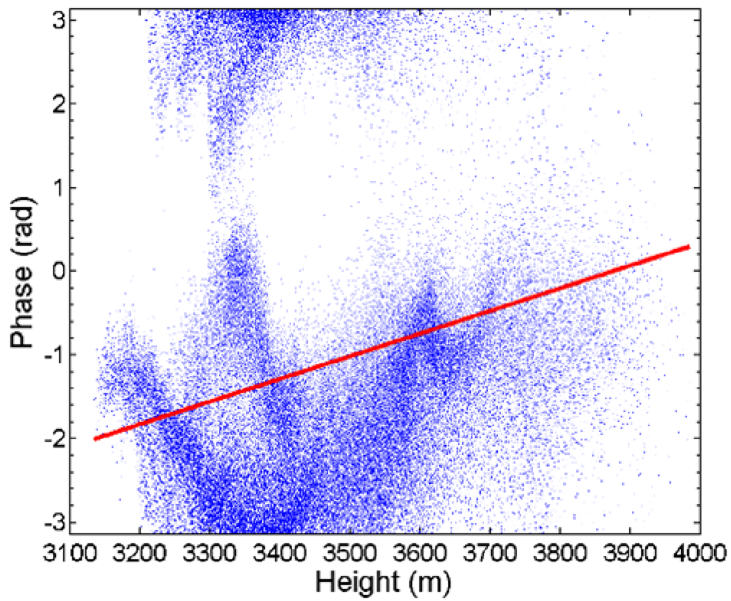

- **The differential phase shows a weak correlation with topography.**

Estimation of turbulent APS

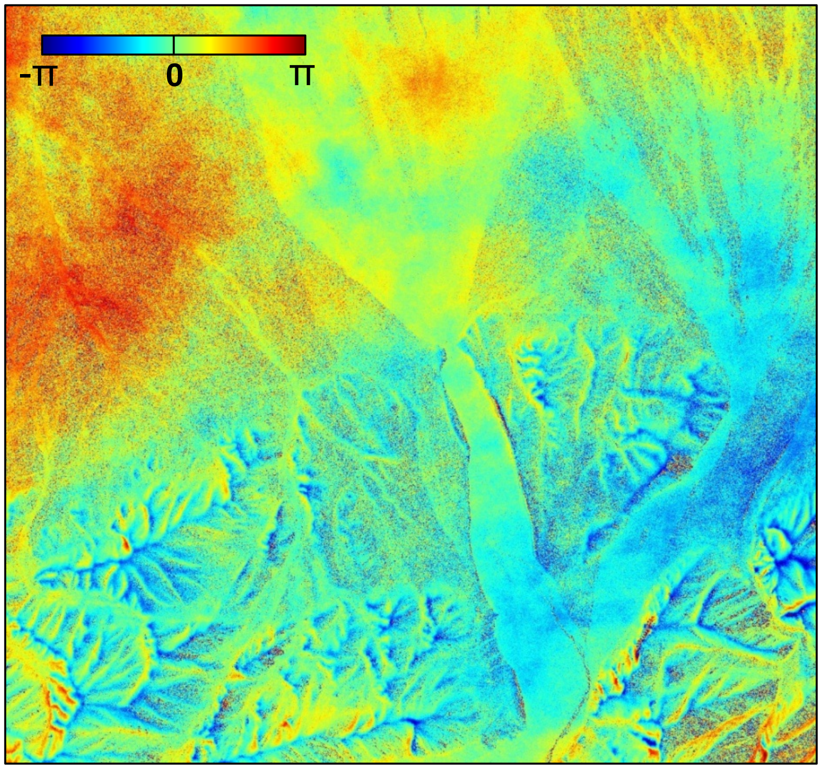

COSMO-SkyMed

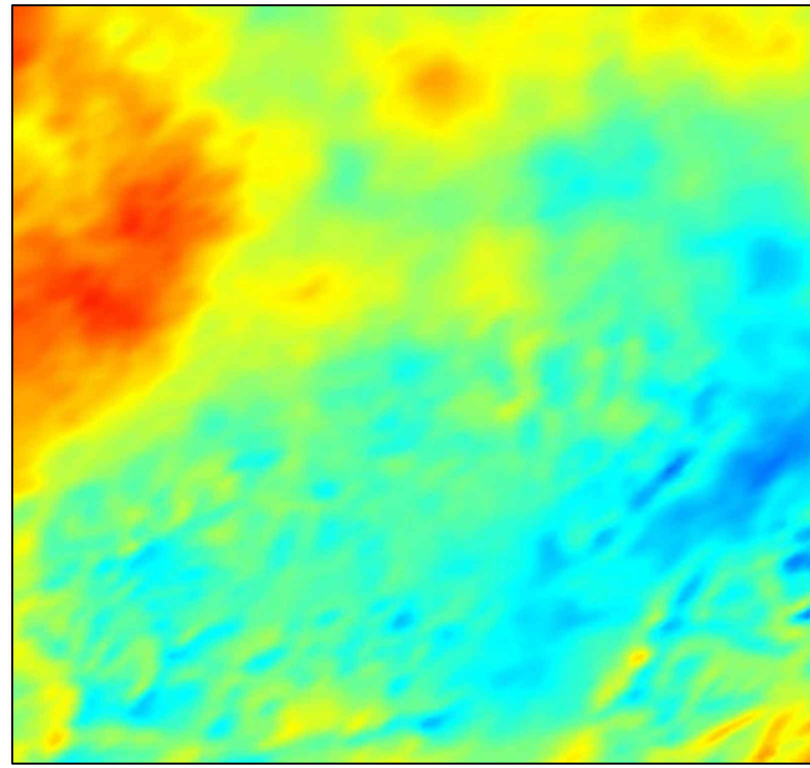

- Based on the result of spatial statistics, the **Kriging interpolation** is used to estimate the **turbulent APS**.

Estimation of turbulent APS

TerraSAR-X

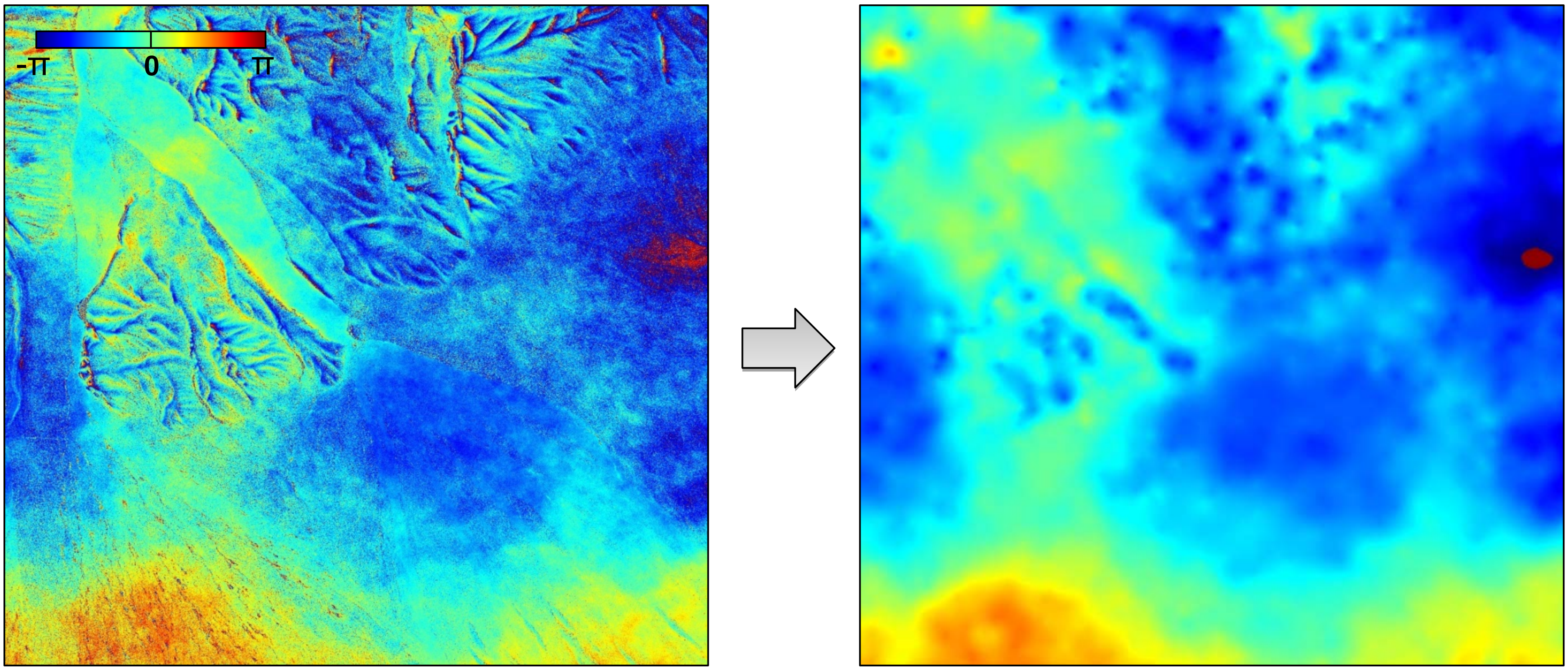

- Based on the result of spatial statistics, the **Kriging interpolation** is used to estimate the **turbulent APS**.

Accuracy improvement by APS removal

Height difference map (COSMO-SkyMed DEM vs. 1:50,000 DEM)

RMS: 13.7m

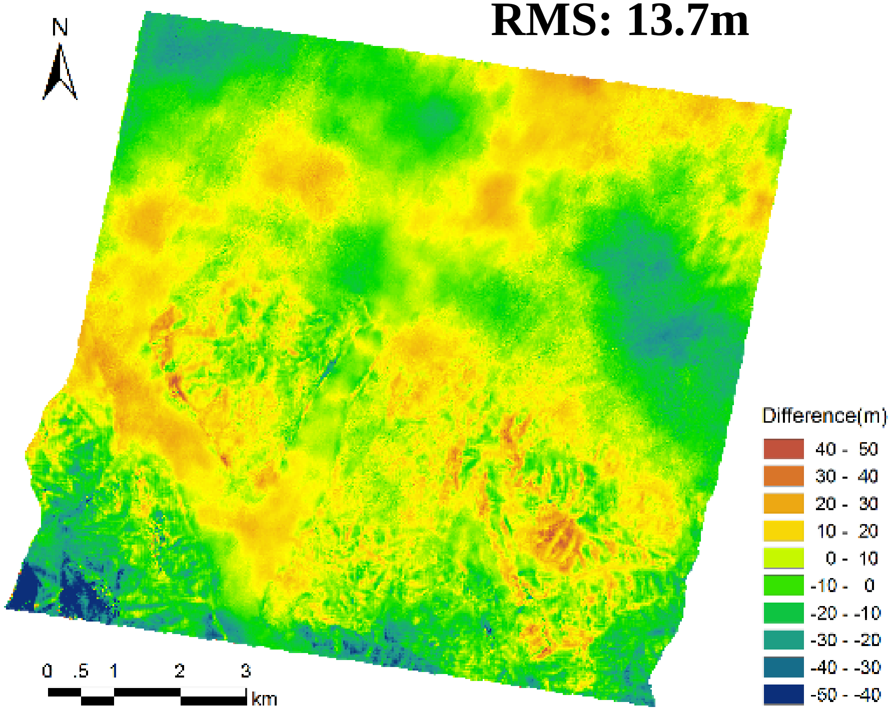

without APS removal

RMS: 5.8m

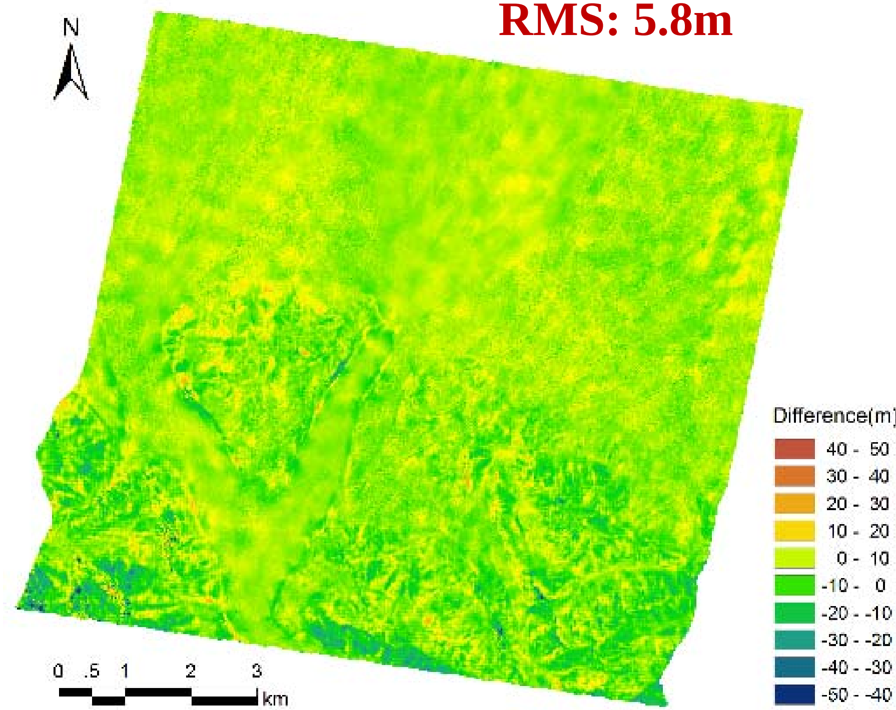

with APS removal

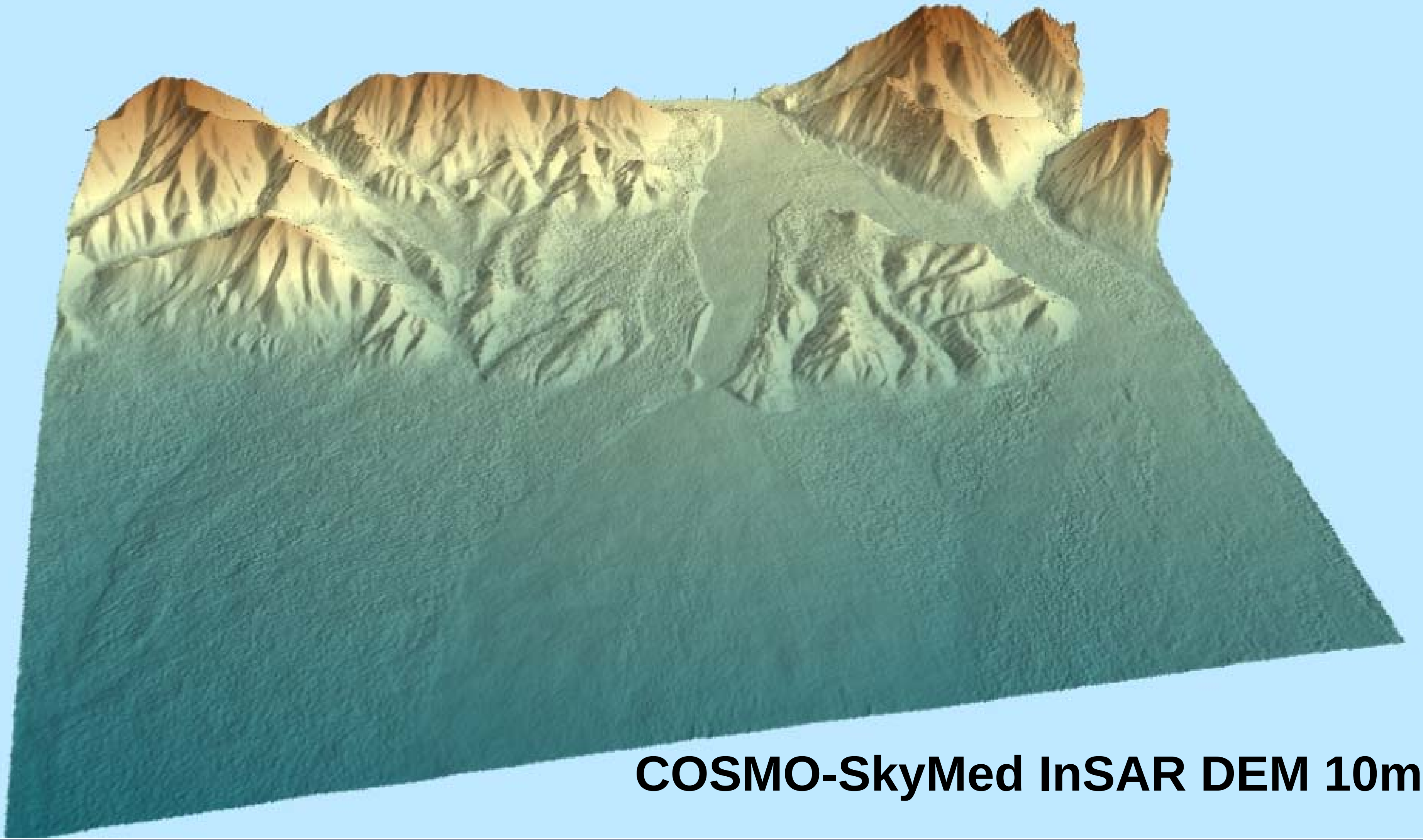

COSMO-SkyMed InSAR DEM 10m

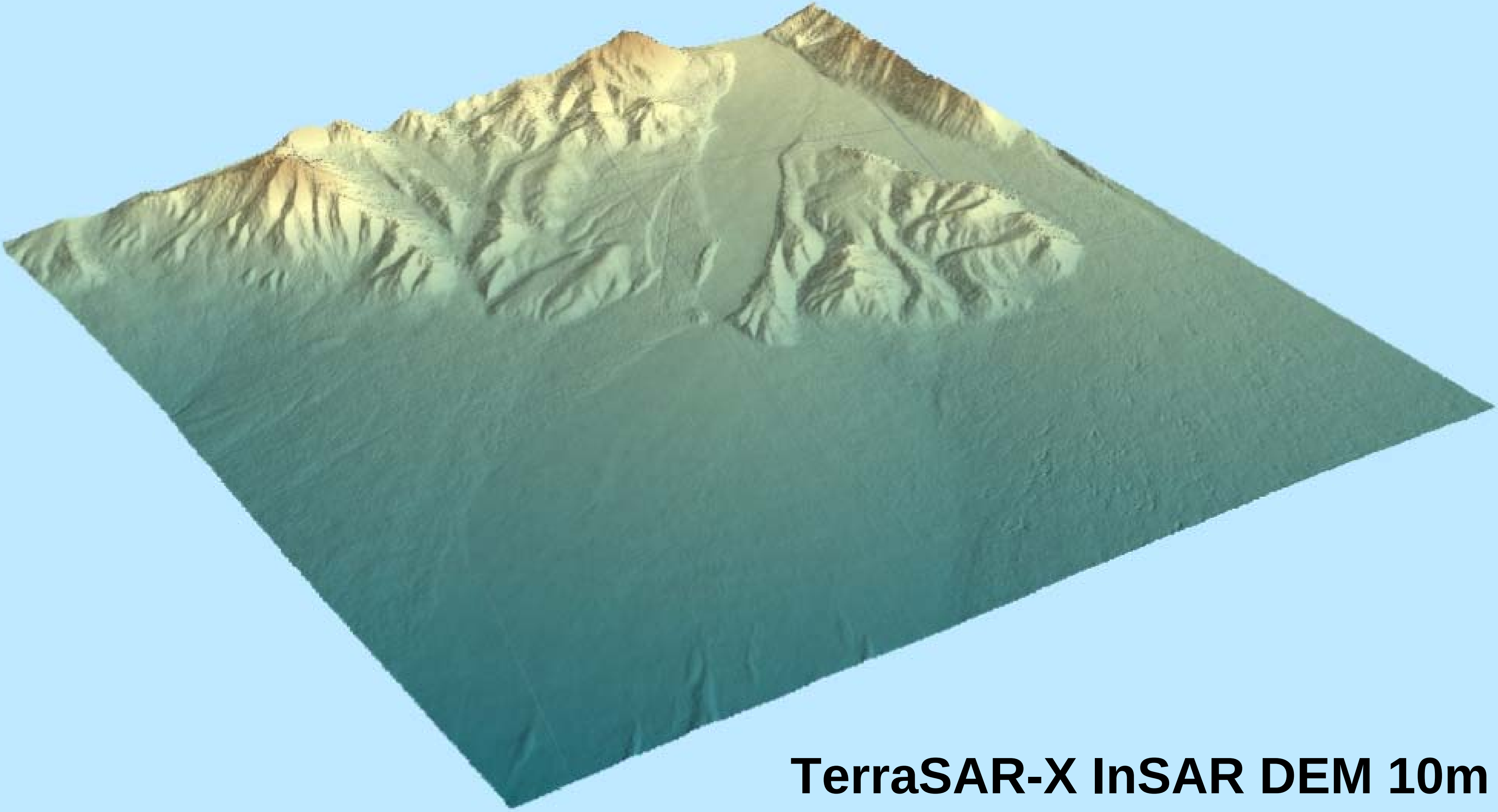

TerraSAR-X InSAR DEM 10m

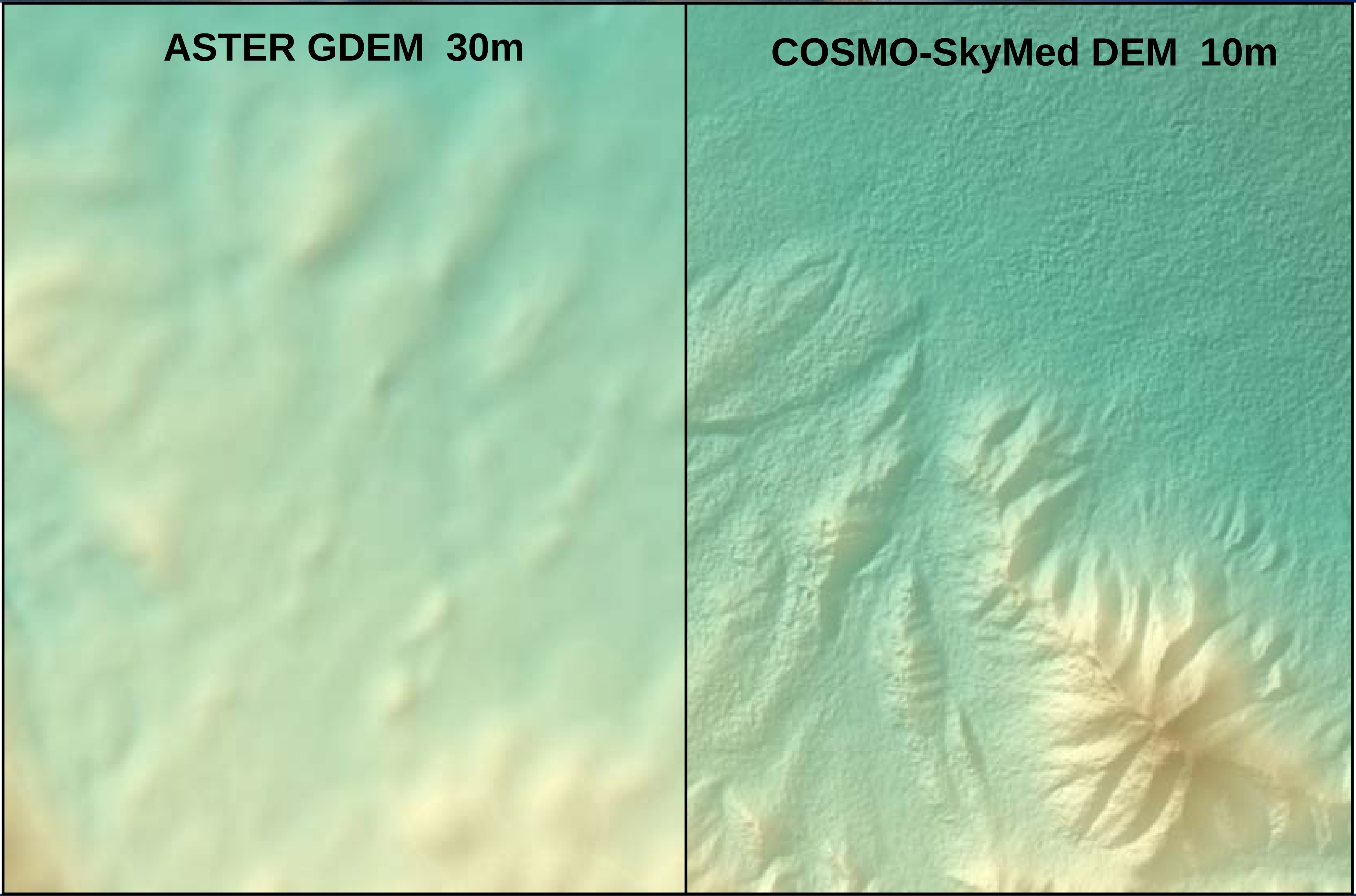
ASTER GDEM 30m
COSMO-SkyMed DEM 10m

DEM Validation

COSMO-SkyMed DEM

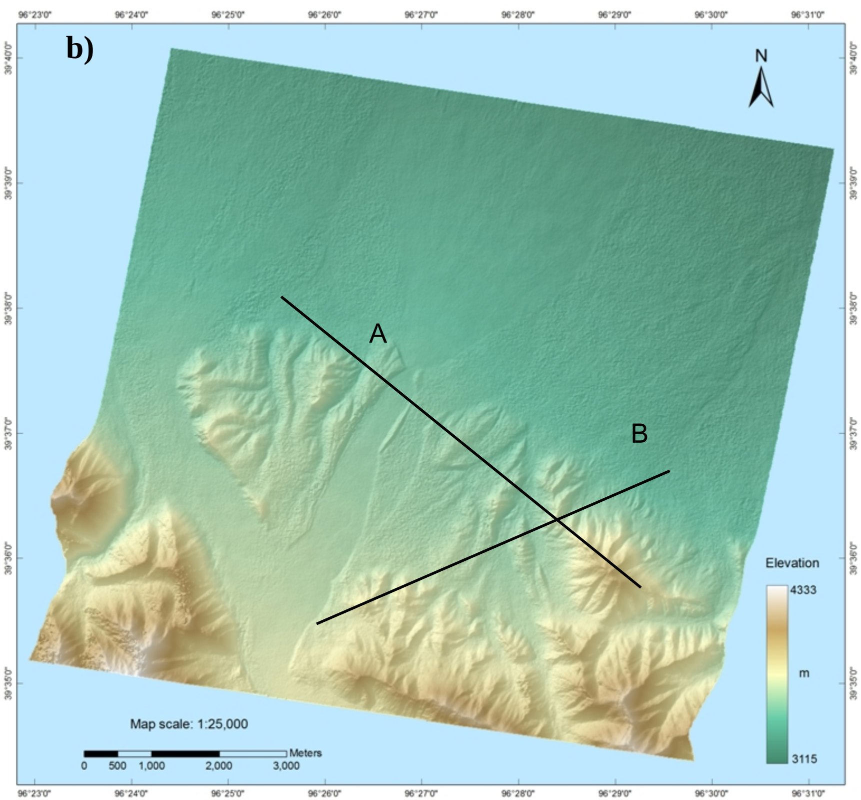

Profile line comparison (vs. 1:50,000 DEM)

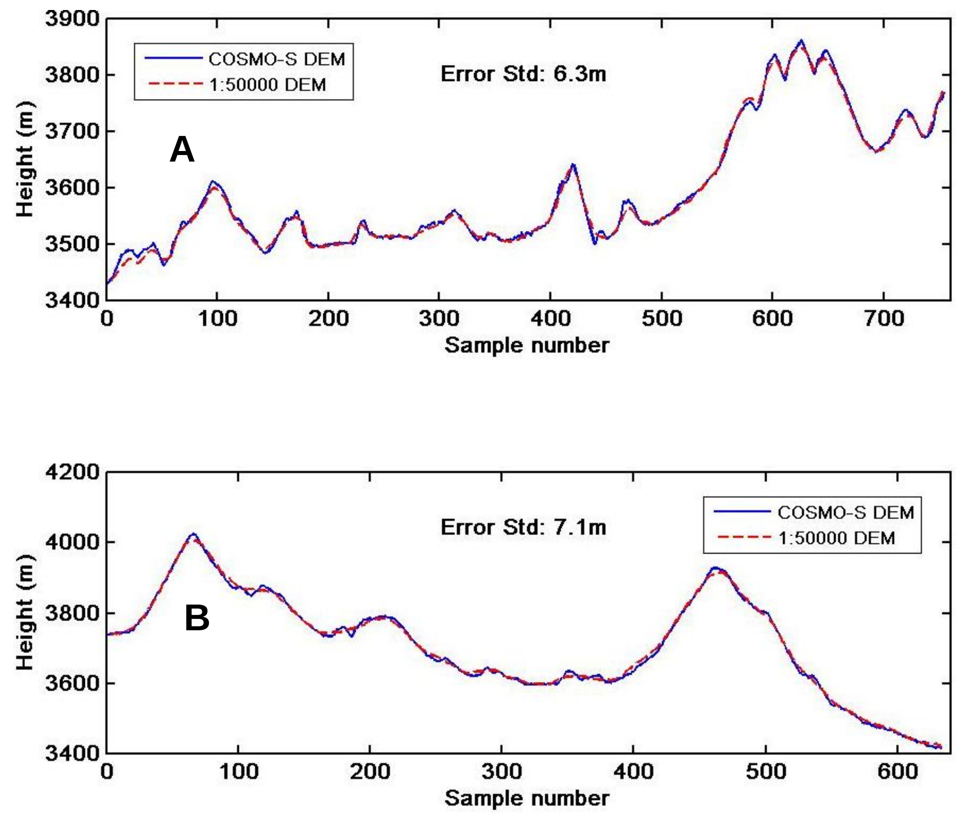

DEM Validation

TerraSAR-X DEM

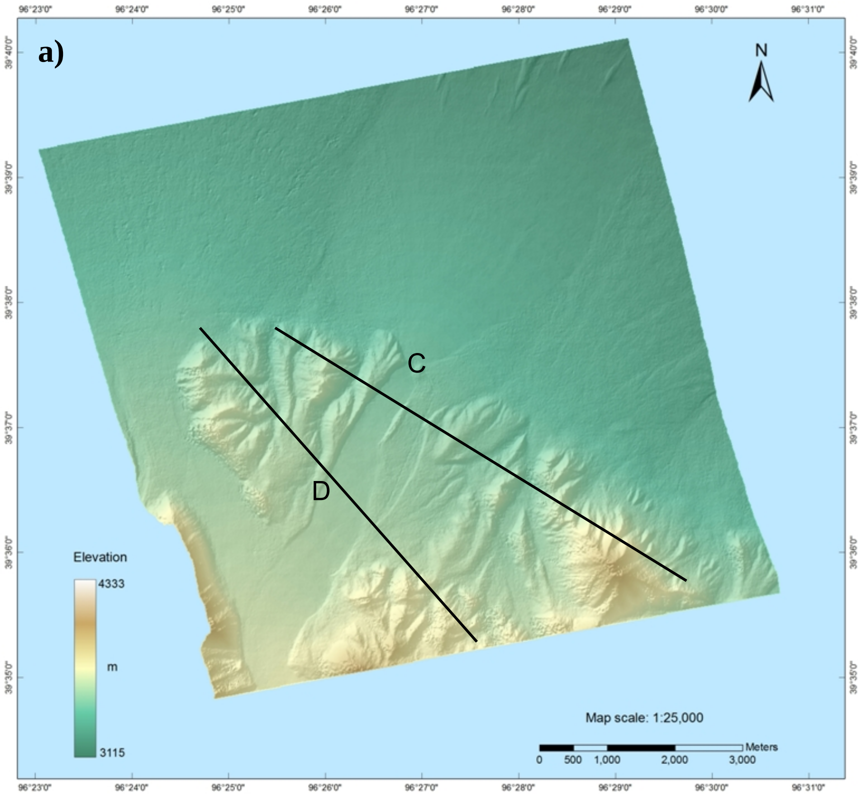

Profile line comparison (vs. 1:50,000 DEM)

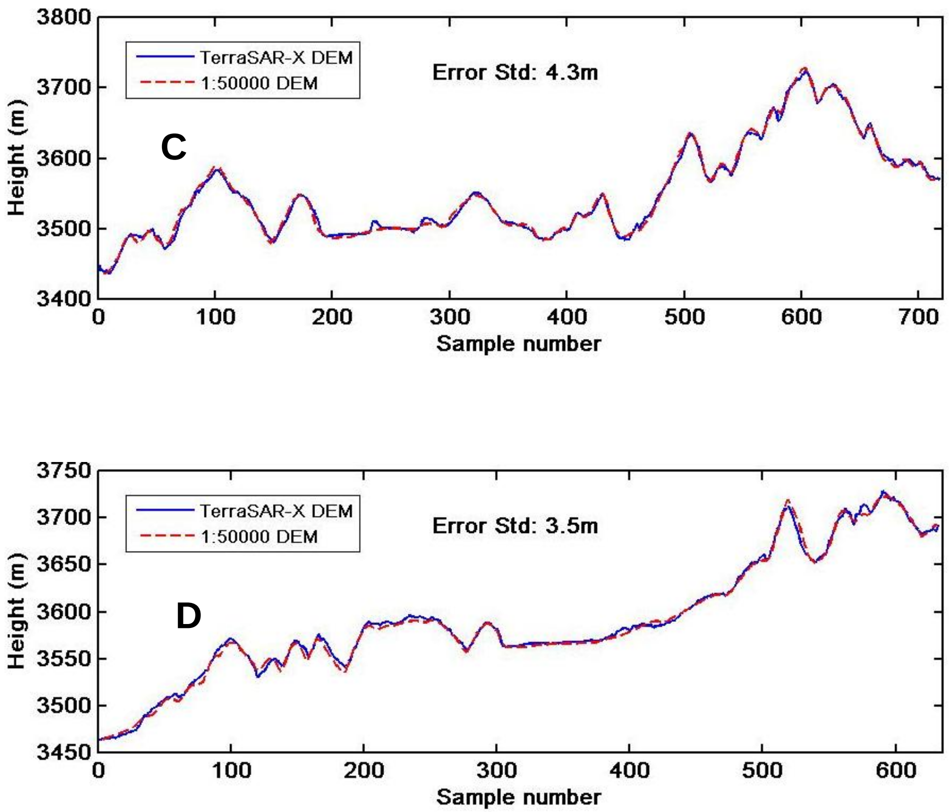

DEM Validation

Height difference statistics on the profile lines

Profile line	Samples	Mean (m)	Std (m)	Abs. error < 5m (%)	Abs. error < 10m (%)
A	301	2.2	**6.2**	60	86
B	249	-0.7	**7.1**	54	84
C	285	-0.2	**4.4**	77	97
D	252	1.1	**3.5**	84	98

High-resolution InSAR DEM may satisfied the DTED-3 standard.

Conclusion & Discussion

- Results from mid-resolution C-band PS-InSAR covering the whole Shanghai city shows the subsidence trend correctly. With ASAR time series datasets we were not only able to detect subsidence zones in the coastal cities, but also at linear features, such as levees.

- Results from high-resolution X-band PS-InSAR, focusing on single constructions, detected uneven subsidence in small areas or at single buildings with detailed deformation distribution.

Conclusion & Discussion

- Multi-frequencies SAR data were applied in 3 Gorges area for monitoring the stability of landslide prone areas. The preliminary results are promising in extracting the deformation with InSAR technique in non-urban areas. More validation and field work are necessary.

- Experimental results with repeat-pass ALOS/PALSAR, COSMO-SkyMed tandem data and TerraSAR-X data show the improvement of InSAR DEM generation. An external DEM is used as reference to remove atmospheric artefacts and to fill data voids in resulting DEM.

Planning and Future Works

- **On the base of the fruitful results from DRAGON-1, the same research team focused on the development of operational PS-InSAR techniques for monitoring land deformation, such as landslides and urban subsidence.**

- **Multi-frequency SAR data sets will be used for future research on InSAR/PS-InSAR. TPM data, such as TerraSAR-X, COSMO-SkyMed and ALOS/PALSAR, has been collected in Shanghai, Three Gorges, Taishan, Ganshu, etc. The investigation will be continued.**

Thank You!